JOC Article

Colorimetric Detection of Cu[II] Cation and Acetate, Benzoate, and Cyanide Anions by Cooperative Receptor Binding in New α,α′-Bis-substituted Donor−Acceptor Ferrocene Sensors

Sara Basurto,[†] Olivier Riant,*[,‡] Daniel Moreno,[†] Josefa Rojo,[†] and Tomás Torroba*[,†]

Química Orgánica, Facultad de Ciencias, Universidad de Burgos, 09001 Burgos, Spain, and Unité de Chimie Organique et Médicinale, Université Catholique de Louvain, Place Louis Pasteur 1, 1348 Louvain-la-Neuve, Belgium

riant@chim.ucl.ac.be; ttorroba@ubu.es

Received February 6, 2007

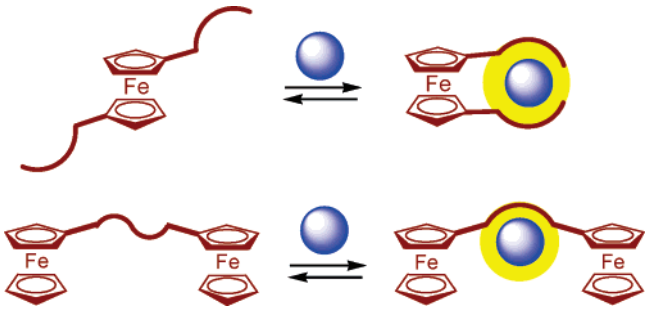

New ferrocene derivatives bearing two donor−acceptor systems are capable of selectively sensing cations and anions by cooperative binding of the two α,α′-groups bonded to the ferrocene nucleus, thus permitting the naked-eye selective colorimetric detection of copper[II] cation and acetate, benzoate, or cyanide anions, which are ions of toxicological and biological relevance.

Introduction

Chemical sensors bearing ferrocene nuclei as part of the sensing unit have been widely studied. Anions sensing by ferrocene bearing sensors has been reported in several reviews that give an accurate idea of the state-of-the-art equipment.[1,2] Electrochemical anion recognition was, by far, the most studied action of ferrocene units appended with secondary amides, including dendrimers with up 18 ferrocene units.[3] Ferrocene along with pyrroles and amide groups has been incorporated in rigid structures in search of selectivity and into silicon, tin, or transition metal containing macrocycles to build electrochemical anion sensors.[4] More recent examples are also known, such as amidoferrocene self-assembled monolayers used for selective electrochemical sensing of anions,[5] or calix[4]arene derivatives containing amide ferrocene units used as electrochemical sensors for carboxylate anions,[6] and tetraza[8]ferrocenophanes that showed spectral and electrochemical anion sensing action with dihydrogen phosphate and fluoride.[7] But, very few ferrocene anion sensors of a chromogenic or fluorogenic nature have been previously reviewed.[8,9] Ferrocene derivatives have been employed for metal ion recognition by means of changes in the

* To whom correspondence should be addressed. (T.T.) Phone: 34-947-258088; fax: 34-947-258087. (O.R.) Phone: +32-(0)10-472740; fax: +32-(0)-10-474168.
[†] University of Burgos.
[‡] Catholic University of Louvain.

(1) (a) Keefe, M. H.; Benkstein, K. D.; Hupp, J. T. *Coord. Chem. Rev.* **2000**, *205*, 201−228. (b) Martínez-Máñez, R.; Sancenón, F. *Chem. Rev.* **2003**, *103*, 4419−4476.

(2) Several examples are included in: (a) Gale, P. A. *Coord. Chem. Rev.* **2000**, *199*, 181−233. (b) Gale, P. A. *Coord. Chem. Rev.* **2001**, *213*, 79−128.

(3) (a) Beer, P. D.; Gale, P. A.; Chen, G. Z. *Coord. Chem. Rev.* **1999**, *204*, 185−186. (b) Beer, P. D.; Cadman, J. *Coord. Chem. Rev.* **2000**, *205*, 131−155. (c) Beer, P. D.; Gale, P. A. *Angew. Chem., Int. Ed.* **2001**, *40*, 486−516 and references therein.

(4) Several examples are found in: (a) Bondy, C. R.; Loeb, S. J. *Coord. Chem. Rev.* **2003**, *240*, 77−99. (b) Gale, P. A. *Coord. Chem. Rev.* **2003**, *240*, 191−221. (c) Sessler, J. L.; Camiolo, S.; Gale, P. A. *Coord. Chem. Rev.* **2003**, *240*, 17−55. (d) Beer, P. D.; Hayes, E. J. *Coord. Chem. Rev.* **2003**, *240*, 167−189.

(5) (a) Beer, P. D.; Davis, J. J.; Drillsma-Milgrom, D. A.; Szemes, F. *Chem. Commun.* **2002**, 1716−1717. (b) Davis, J. J. *Chem. Commun.* **2005**, 3509−3513.

(6) Tomapatanaget, B.; Tuntulani, T.; Chailapakul, O. *Org. Lett.* **2003**, *5*, 1539−1542.

(7) Otón, F.; Tárraga, A.; Espinosa, A.; Velasco, M. D.; Bautista, D.; Molina, P. *J. Org. Chem.* **2005**, *70*, 6603−6608.

(8) Selected examples in: Suksai, C.; Tuntulani, T. *Chem. Soc. Rev.* **2003**, *32*, 192−202.

10.1021/jo0702589 CCC: $37.00
Published on Web 05/25/2007

electrochemical response of the host molecule. Usually, cation binding at an adjacent receptor site induces a positive shift in the redox potential of the ferrocene−ferrocenium couple by electrostatic interactions. By varying the applied potential, the complexing ability of the ligand can be switched on and off. Bis-ferrocenyl systems containing an imidazoline unit have been employed for this purpose.[10] Metal ion sensing has been studied in ferrocene criptands and bis-dipicolylaminoferrocene derivatives by coupling the redox response and the redox switched complexation of both ferrocene derivatives.[11] A ferrocene−cyclam derivative has been used as a redox active macrocycle for the complexation of transition metal cations,[12] and a crown ether containing amidoferrocence receptor showed positive cooperative binding toward a bromide anion in the presence of a sodium ion by ^{1}H NMR and electrochemic evaluation.[13]

Ferrocenophane derivatives have been studied as electrochemical sensors of the magnesium[II] ion, also giving highly visual output responses.[14] Especially remarkable is the case of an electroactive nitrogen-rich [4.4]ferrocenophane displaying selective sensing of magnesium[II] ions that worked as a redox switchable ion carrier.[15] The reports of ferrocene receptors for organic molecules, charged or neutral, are less common. By incorporation of the redox active ferrocene unit into receptors containing 2,6-diaminopyridine units, novel ferrocene receptors for barbiturates and ureas have been described.[16] In the same way, ferrocene bis-amidopyridine receptors were able to bind dicarboxylic acids by hydrogen bonding interactions,[17] and a ferrocene-based bis(*o*-trifluoroacetylcarboxanilide) receptor selectively recognized electrochemically *m*-phenylene diacetate through cooperative binding.[18] Electrochemical sensing of neutral species has been performed by a ferrocene−porphyrin conjugate,[19] and electrochemical detection of saccharides was performed by ferroceneboronic acid derivatives.[20] Ferrocene sensors based in purely optical detection are an emerging area that is providing new data. Ferrocene has been used as a donor system in conjugated, extended push−pull compounds, and their ability to bind metal cations, such as magnesium[II] or europium[III], has been studied by UV/vis spectrophotometric titrations.[21] A ferrocene−anthracene-linked dyad showing selective fluorescence enhancement upon binding to lithium cations has been characterized.[22] A novel linear triferrocene derivative bearing two azadiene bridges has been shown to be a specific optical and electrochemical sensor for magnesium[II] cations, forming a 1:1 complex that can be used for naked-eye detection[23] and a bis-guanidine[3.3]ferrocenophane sensor that displayed metal ion recognition by fluorescence measurements.[24] A difunctionalized naphthalene aza-ferrocenophane showed a fluorescent response to the fluoride anion,[25] and a ferrocene-based ditopic receptor containing urea and benzocrown ether units showed color changes in the presence of fluoride anions that disappeared in the presence of potassium cations, therefore permitting on−off switching.[26]

SCHEME 1

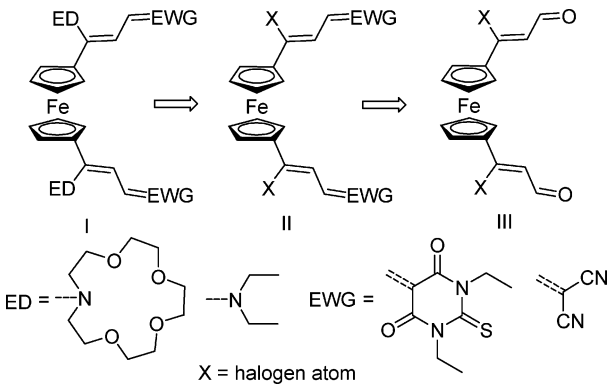

The pivotal capacity of the ferrocene nucleus to take part in the sensing action as spacers and donors reinforced the optical response of certain receptor systems. In this way, bis-substituted ferrocene compounds bearing multiple amido groups selectively detected $H_2PO_4^-$ ions,[27] and a bis-substituted ferrocene with multipoint binding sites showed strong 1:1 binding to unprotected α-amino acids.[28] These two cases showed remarkable optical responses by UV−vis and fluorescence. With the aim of preparing new optical sensors for cations and anions of environmental importance, we designed new 1,1′-bis-substituted ditopic ferrocene receptors bearing conjugated donor and acceptor groups and permitting structural diversity. In our projected systems, the ferrocene nucleus will act both as rotating spacer and donor group, thus allowing cooperative binding of α,α′-substituents. The retrosynthetic pathway for the design of the new structures is shown in Scheme 1. Compounds with the general structure **I**, having dimethylamino or aza-crown ether donors and some acceptor groups such as thiobarbiturylidene or dicyanoalkylidene groups, are well-suited for complexation schemes and can be easily accessed from the halovinylidene

(9) Some examples in: Martínez-Máñez, R.; Sancenón, F. *J. Fluoresc.* **2005**, *15*, 267−285.
(10) Sutcliffe, O. B.; Bryce, M. R.; Batsanov, A. S. *J. Organomet. Chem.* **2002**, *656*, 211−216 and references therein.
(11) (a) Plenio, H.; Aberle, C. *Chem.—Eur. J.* **2001**, *7*, 4438−4446. (b) Siemeling, U.; Auch, T. C. *Chem. Soc. Rev.* **2005**, *34*, 584−594.
(12) Plenio, H.; Aberle, C.; Al Shihadeh, Y.; Lloris, J. M.; Martínez-Máñez, R.; Pardo, T.; Soto, J. *Chem.—Eur. J* **2001**, *7*, 2848−2861.
(13) Suksai, C.; Leeladee, P.; Jainuknan, D.; Tuntulani, T.; Muangsin, N.; Chailapakul, O.; Kongsaereeb, P.; Pakavatchaic, C. *Tetrahedron Lett.* **2005**, *46*, 2765−2769.
(14) (a) Tárraga, A.; Molina, P.; López, J. L.; Velasco, M. D. *Tetrahedron Lett.* **2003**, *44*, 3371−3375. (b) Tárraga, A.; Molina, P.; López, J. L.; Velasco, M. D. *Dalton Trans.* **2004**, 1159−1165. (c) López, J. L.; Tárraga, A.; Espinosa, A.; Velasco, M. D.; Molina, P.; Lloveras, V.; Vidal-Gancedo, J.; Rovira, C.; Veciana, J.; Evans, D. J.; Wurst, K. *Chem.—Eur. J* **2004**, *10*, 1815−1826. (d) Li, M.; Cai, P.; Duan, C.; Lu, F.; Xie, J.; Meng, Q. *Inorg. Chem.* **2004**, *43*, 5174−5176.
(15) Caballero, A.; Lloveras, V.; Tárraga, A.; Espinosa, A.; Velasco, M. D.; Vidal-Gancedo, J.; Rovira, C.; Wurst, K.; Molina, P.; Veciana, J. *Angew. Chem., Int. Ed.* **2005**, *44*, 1977−1981.
(16) Collinson, S. R.; Gelbrich, T.; Hursthouse, M. B.; Tucker, J. H. R. *Chem. Commun.* **2001**, 555−556.
(17) (a) Carr, J. D.; Coles, S. J.; Hursthouse, M. B.; Light, M. E.; Tucker, J. H. R.; Westwood, J. *Angew. Chem., Int. Ed.* **2000**, *39*, 3296−3299. (b) Tucker, J. H. R.; Collinson, S. R. *Chem. Soc. Rev.* **2002**, *31*, 147−156 and references therein.
(18) Kim, D.; Miyaji, H.; Chang, B.-Y.; Park, S.-M.; Ahn, K. H. *Chem. Commun.* **2006**, 3314−3316.
(19) Bucher, C.; Devillers, C. H.; Moutet, J. C.; Royal, G.; Saint-Aman, E. *Chem. Commun.* **2003**, 888−889.
(20) Arimori, S.; Ushiroda, S.; Peter, L. M.; Jenkins, A. T. A.; James, T. D. *Chem. Commun.* **2002**, 2368−2369 and references therein.
(21) Pasini, D.; Righetti, P. P.; Rossi, V. *Org. Lett.* **2002**, *4*, 23−26.
(22) Caballero, A.; Tormos, R.; Espinosa, A.; Velasco, M. D.; Tárraga, A.; Miranda, M. A.; Molina, P. *Org. Lett.* **2004**, *6*, 4599−4602.
(23) Caballero, A.; Tárraga, A.; Velasco, M. D.; Espinosa, A.; Molina, P. *Org. Lett.* **2005**, *7*, 3171−3174.
(24) Otón, F.; Tárraga, A.; Molina, P. *Org. Lett.* **2006**, *8*, 2107−2110.
(25) Otón, F.; Tárraga, A.; Velasco, M. D.; Espinosa, A.; Molina, P. *Chem. Commun.* **2004**, 1658−1659.
(26) Miyaji, H.; Collinson, S. R.; Prokês, I.; Tucker, J. H. R. *Chem. Commun.* **2003**, 64−65.
(27) Kuo, L.-J.; Liao, J.-H.; Chen, C.-T.; Huang, C.-H.; Chen, C.-S.; Fang, J.-M. *Org. Lett.* **2003**, *5*, 1821−1824.
(28) Debroy, P.; Banerjee, M.; Prasad, M.; Moulik, S. P.; Roy, S. *Org. Lett.* **2005**, *7*, 403−406.

SCHEME 2

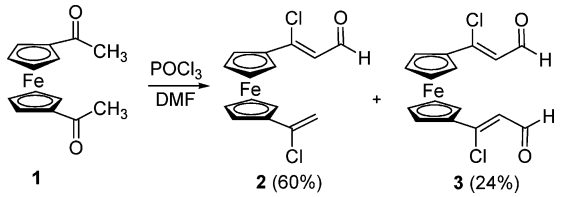

SCHEME 3

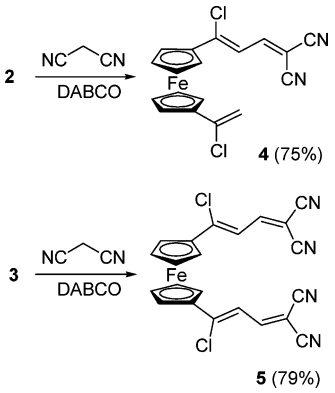

derivatives **II**, which in turn may be obtained from 1,1′-bis(2-formyl-1-halovinyl)ferrocene **III**. In this paper, we report a complete study of the binding ability of compounds of type **I** and their selectivity in the detection of transition metal cations and biologically relevant anions.

Results and Discussion

Synthesis of the New Receptors. Precursor **III** was obtained following literature procedures.[29] The reported methodologies showed some disagreements in the description of the products and yields of similar reactions. In our hands, treatment of diacetylferrocene[30] **1** (1 equiv) with the Vilsmeier reagent [$POCl_3$ in dimethylformamide (DMF), 6 equiv], following the standard procedure, afforded, after column chromatography, 1-(2-formyl-1-chlorovinyl)-1′-(1-chlorovinyl)ferrocene **2** as the main product (60%) and the expected 1,1′-bis(2-formyl-1-chlorovinyl)ferrocene **3** in lower yield (24%). Compound **2** was moderately stable and could be stored in the dark at −20 °C for several days to weeks, but compound **3** resulted in being rather unstable and could be stored in the dark at −20 °C only for a few hours; therefore, it was used freshly prepared every time it was required (Scheme 2).

Compounds **2** and **3** (1 equiv) were treated independently with malononitrile (3 equiv) in the presence of 1,4-diazabicyclo-[2.2.2]octane (DABCO, 3 equiv), in dichloromethane at room temperature for 5−15 min. Workup and column chromatography afforded, respectively, compounds **4** (75%) and **5** (79%) as deep blue stable solids at room temperature (Scheme 3).

In the same way, compounds **2** and **3** were treated independently with 1,3-diethyl-2-thiobarbituric acid (3 equiv) and

SCHEME 4

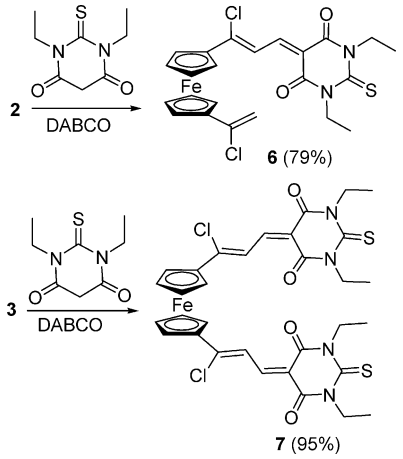

SCHEME 5

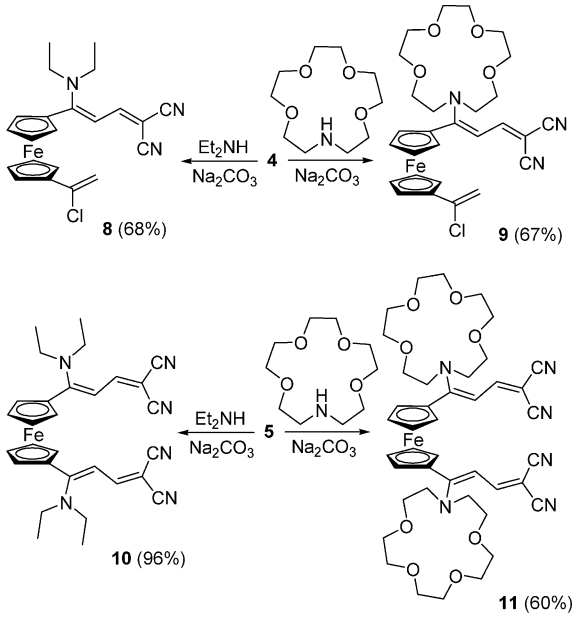

DABCO (3 equiv), in dichloromethane at room temperature for 5−15 min. Workup and column chromatography as before afforded, respectively, compounds **6** (79%) and **7** (95%) as deep green stable solids (Scheme 4).

Compounds **4**−**7** were subsequently treated independently with dimethylamine or 1-aza-15-crown-5 ether (2 equiv) in the presence of Na_2CO_3 (3 equiv) in dichloromethane at room temperature for 2−24 h. Workup and flash column chromatography of the reaction residues afforded compounds **8**−**15** in 60−97% yields as orange stable solids (Schemes 5−7).

Compounds **4**−**7** were next treated independently with 1,-15-diphenyl-2,14-diaza-5,8,11-trioxapentadecane **16**[31] in different solvents (dichloromethane, acetonitrile, tetrahydrofurane (THF), and THF/H_2O) and in the presence of different bases (Na_2CO_3, K_2CO_3, Cs_2CO_3, and NaOH). Compounds **4**−, **5**, and **7** decomposed in all reaction conditions we employed, but treatment of **6** (1.5 equiv) with **16** (1 equiv), in the presence of Na_2CO_3 (5 equiv), in THF/H_2O 3:1 at room temperature for 20 min afforded, after aqueous acid workup and column

(29) (a) Puciová, M.; Solèániová, E.; Pronayová, N.; Loos, D.; Toma, Š. *Tetrahedron* **1993**, *49*, 7733−7742. (b) Rosenblum, M.; Brawn, N.; Papenmeier, J.; Applebaum, M. *J. Organomet. Chem.* **1966**, *6*, 173−180. (c) Seideimann, O.; Beyer, L.; Richter, R.; Herr, T. *Inorg. Chim. Acta* **1998**, *271*, 40−48. (d) Schottenberger, H.; Lukassser, J.; Reichel, E.; Müller, A. G.; Steiner, G.; Kopacka, H.; Wurst, K.; Ongania, K. H.; Kirchner, K. *J. Organomet. Chem.* **2001**, *637*−*639*, 558−576.

(30) Rausch, M. D.; Fischer, E. O.; Grubert, H. *J. Am. Chem. Soc.* **1960**, *82*, 76−82.

(31) Krakowiak, K. E.; Bradshaw, V.; Izatt, R. M. *J. Org. Chem.* **1990**, *55*, 3364−3368.

SCHEME 6

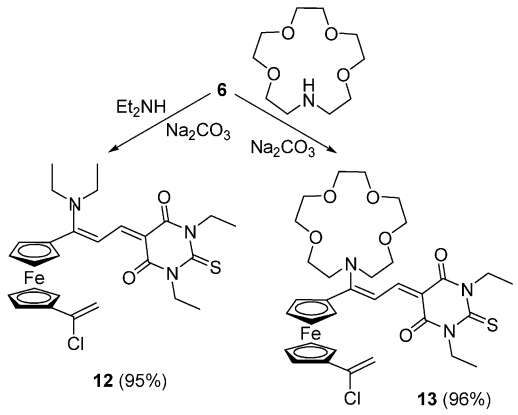

SCHEME 7

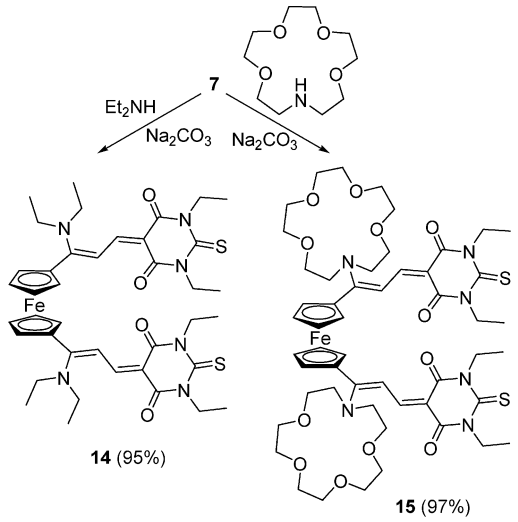

SCHEME 8

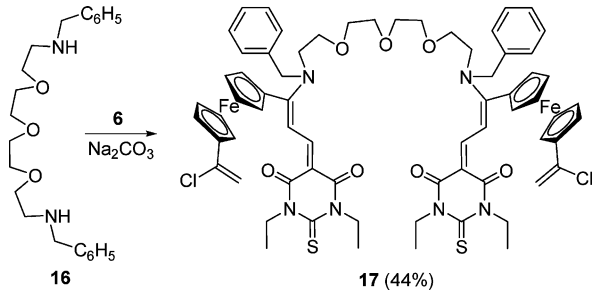

chromatography, bis-ferrocenyldiamine **17** (44%) as an orange stable solid (Scheme 8).

All new compounds **4**−**15** and **17** were characterized by the usual spectroscopic and analytical techniques, IR, UV, ^{1}H or−^{13}C NMR, DEPT of selected examples, etc. LC/MS (APCI) was used to proof the correct molecular weight of compounds because the usual techniques of mass spectrometry, such as EI-MS or EI-HRMS, did not afford the molecular peak signal.

Titration Experiments. During the preliminary preparation of solutions of the prepared compounds **8**−**15** and **17**, to check their suitability as new chemical sensors, we noticed that compounds **8**−**11**, bearing a dicyanovinyl unit, were scarcely soluble in acetonitrile, the solvent of choice for cation complexation tests, and that the solutions were not completely stable for a long time under normal conditions, affording sometimes unrepeatable experimental results. Therefore, we concentrated our efforts in the study of compounds **12**−**15** and **17**, bearing a *N*,*N*-diethylthiobarbituric unit, that conferred sufficient solubility in dilute acetonitrile solutions and that were stable in normal conditions and afforded repeatable results. All these compounds showed an intense UV−vis spectral band with its maximum centered at 443−448 nm, which was responsible for the strong yellow color of their solutions. They also showed very high value molar extinction coefficients. For these compounds, λ_{max} (nm) and $\epsilon \times 10^4$ (M^{-1} cm^{-1}) (in parentheses) were as follows: **12**, 442 (9.04); **13**, 447 (15.22); **14**, 443 (10.71); **15**, 448 (14.86); and **17**, 448 (9.70). This absorption band is apparently due to the charge transfer between the amine group and the thiobarbituric moiety. The fact that derivatives having one or two conjugated units showed similar absorption bands indicated that the crossed conjugation across the ferrocene group had very little influence on the main absorption band. This fact made these compounds suitable for interactions based on perturbation of the conjugation by interaction with any of the units that were involved in the charge-transfer band. We therefore decided to test the sensitivity of these compounds to the presence of the most usual cations as perchlorate or triflate salts in acetonitrile solution (see Supporting Information for experimental details). To study the cooperative binding of the two α,α′-groups present in compounds **14**−**15**, we performed a comparative study of the behavior of these compounds in contrast to the corresponding monosubstituted derivatives **12**−**13**. In preliminary experiments, 10^{-5} M solutions of **12**−**15** decolorized almost totally in the presence of 2 equiv of Cu^{2+}, although discoloration in the presence of Cu^{2+} was less evident in the case of **17** than in the other cases. The color of all the compounds remained in the presence of 2 equiv of each one of the other cations. The presence of common alkali metals or alkaline earth metal cations had no influence on the studied compounds. A representative example is given in Figure 1 that shows the effect of the addition of 2 equiv of every cation used in this study to a 10^{-5} M solution of **14**. The effect was similar for **12**− and **13** and **15**, independently of the structural variations of every compound. As can be seen in Figure 1, these compounds permit the naked-eye selective detection of the presence of copper[II] in acetonitrile.

The UV−vis spectra of compounds **12**−**15** and **17** (Figure 2 and Figures S1−S4 in the Supporting Information), in the presence of 2 equiv of the same cations in acetonitrile, showed changes according to the qualitative colorimetric experiments. Thus, almost extinction of the 442−448 nm band of the UV−vis spectra of every compound, in the presence of 2 equiv of Cu^{2+}, was detected, and a partial extinction of the main absorption band of every compound in the presence of Hg^{2+} and Fe^{3+}, which was not appreciated by the naked-eye inspection of the corresponding solutions, was also detected. Compound **14** was the most selective compound (Figure 2) and showed very little attenuation at 442−448 nm in the presence of 2 equiv of Fe^{3+}. Compound **15** (Figure S3 in the Supporting Information) showed significant attenuation in the presence of 2 equiv of Fe^{3+}, and although second best, it was a long way behind **14** and not so different from the other receptors in the presence of Fe^{3+}. The less selective compound was **17** (Figure S4 in the Supporting Information), where the presence of 2 equiv of either Cu^{2+}, Hg^{2+}, or Fe^{3+} conducted a large attenuation of the 448 nm spectral band, although the compound was affected to a bigger proportion by the presence of Cu^{2+}. The effect of the

Ligand, Zn^{2+}, Cd^{2+}, Sc^{3+}, Ag^{+}, Hg^{2+}, Sn^{2+}, Ni^{2+}, Pb^{2+}, Al^{3+}, Fe^{3+}, Cu^{2+}

FIGURE 1. Effect of the addition of 2 equiv of every indicated cation to a 10^{-5} M solution of **14** in acetonitrile.

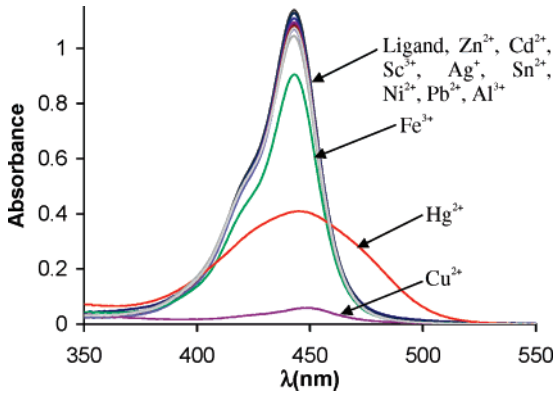

FIGURE 2. UV−vis spectrum of **14** (10^{-5} M, CH_3CN) in the presence of 2 equiv of every cation.

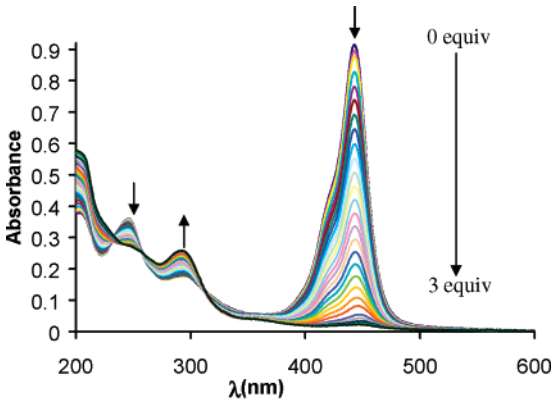

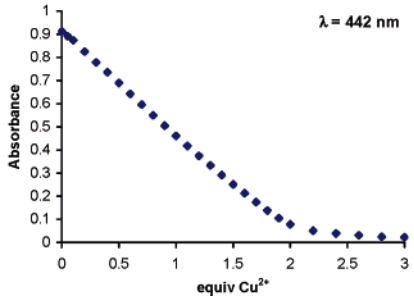

FIGURE 3. UV−vis titration of **12** (10^{-5} M, CH_3CN) in the presence of Cu^{2+} and representation of the variation of absorbance at 442 nm with respect to equiv of Cu^{2+}.

presence of 2 equiv of Hg^{2+} was similar in all compounds, giving rise to attenuation and enlargement of the intensity of the absorption band; therefore, the complexation mechanism in this case could be different from the interactions shown by the presence of the other cations.

In view of the close similarity of the response of all compounds studied, but especially **12**−**15**, to the presence of the same number of equivalents of the same cations, we performed accurate titrations of 10^{-5} M solutions in acetonitrile of every compound by addition of increasing amounts of concentrated acetonitrile solutions of perchlorate or triflate salts of every active cation, taking the UV−vis spectrum of all additions and representing the variation of the maximum wave absorption with respect to the number of added equivalents of every studied cation. Taking in account that the structures of **12** and **14**, in one hand, and **13** and **15**, on the other hand, are closely related, the comparison of their respective titration behavior may give clues about their mechanism and sensitivity. The most interesting response of all compounds was reported for the presence of copper[II]; therefore, we first performed the titration of the compounds and Cu^{2+}.

The UV−vis titration representations in Figures 3−7 showed the presence of some isosbestic points, but several differences between them, as well as the differences between the plots of absorbance versus equiv of Cu^{2+}, gave clues about the type of complexation in each case. UV−vis titration of **12** showed a gradual extinction of the 442 nm signal in the presence of increasing amounts of Cu^{2+}, a small increase of the 286 nm signal, and a small decrease of the 244 nm signal. Three isosbestic points were visible, two of them at 311 and 255 nm that remain unchanged during the titration, and another one at 228 nm, which were kept until the second equivalent of Cu^{2+} was added but then was lost due to the excess Cu^{2+} present in the solution. Therefore, a unique species formed in the equilibrium of the titration, the stoichiometry of which is given by the representation of the variation of absorbance at 442 nm with respect to equiv of Cu^{2+}. Effectively, the absorbance at 442 nm decreases constantly until the addition of 2 equiv of Cu^{2+}, and further amounts of Cu^{2+} induce only very minor changes in the absorbance; therefore, a M_2L complex seems to be formed during the titration. Analogously, the UV−vis titration of **13** showed a gradual extinction of the 447 nm signal between 0 and 2 equiv of Cu^{2+}, but this time, the mechanism appeared slightly different because the representation of the variation of absorbance at 447 nm with respect to equiv of Cu^{2+} showed the presence of two regions with different slopes, which is probably due to the presence of two different species, ML and M_2L, formed by the addition of 1 and 2 equiv of Cu^{2+}. Two isosbestic points at 308 and 349 nm were detected between 0 and 1 equiv of Cu^{2+}, and three more isosbestic points at 235, 247, and 367 nm were detected between 1 and 2 equiv of Cu^{2+}, confirming the formation of the two species. The presence of an aza-crown ether probably drove the formation of a first 1:1 complex, and once complexed, the thione group formed a second complex with an additional Cu^{2+} cation.

UV−vis titration of **14** showed the presence of an isosbestic point at 230 nm, which was observed during all the titration experiments, and two additional isosbestic points at 263 and 300 nm, only visible until the addition of the first equivalent of Cu^{2+}. The representation of the variation of absorbance at 443 nm with respect to equiv of Cu^{2+} showed two regions with different slopes, one of them between 0 and 1 equiv and another

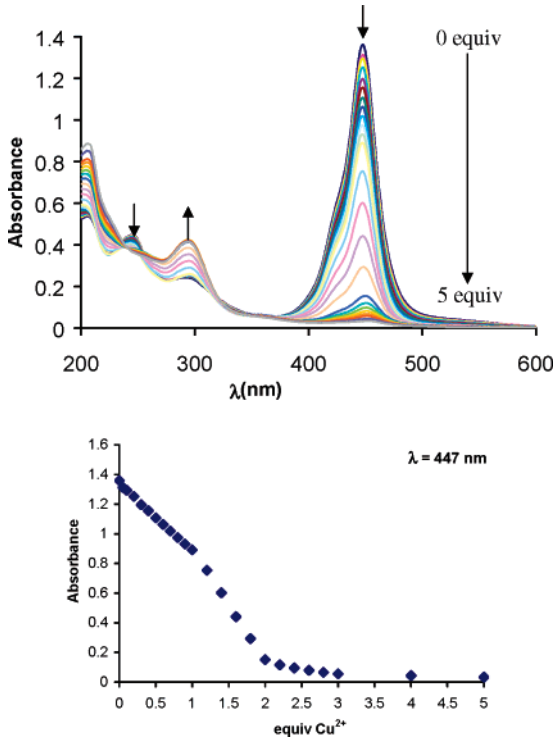

FIGURE 4. UV−vis titration of **13** (10^{-5} M, CH_3CN) in the presence of Cu^{2+} and representation of the variation of absorbance at 447 nm with respect to equiv of Cu^{2+}.

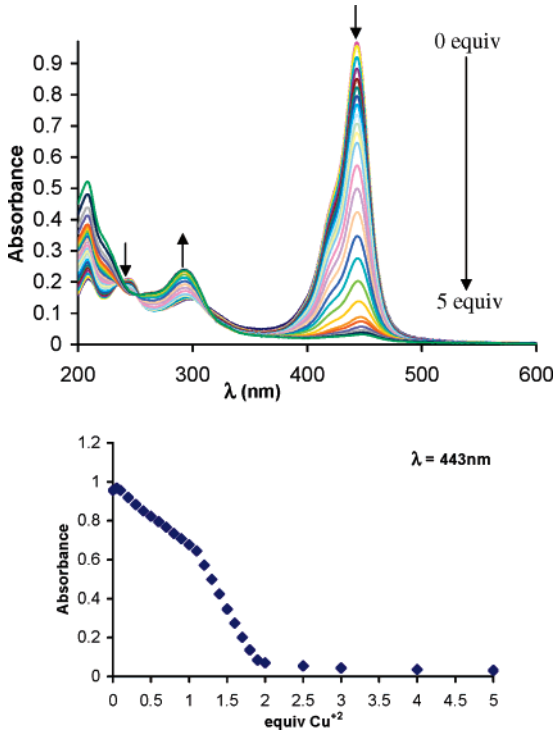

FIGURE 5. UV−vis titration of **14** (10^{-5} M, CH_3CN) in the presence of Cu^{2+} and representation of the variation of absorbance at 443 nm with respect to equiv of Cu^{2+}.

one between 1 and 2 equiv of Cu^{2+}. Apparently, two different species were formed, one of them between 0 and 1 equiv and another one between 1 and 2 equiv of Cu^{2+}. After the addition of 2 equiv of Cu^{2+}, the extinction of the band at 443 nm was

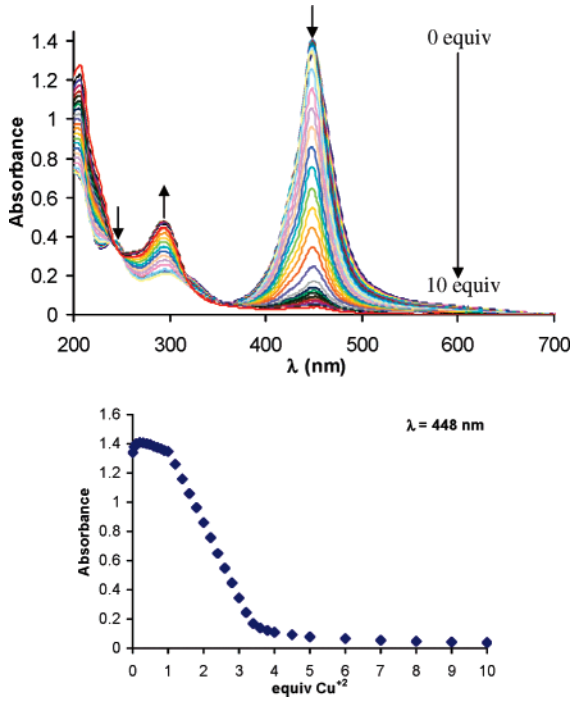

FIGURE 6. UV−vis titration of **15** (10^{-5} M, CH_3CN) in the presence of Cu^{2+} and representation of the variation of absorbance at 448 nm with respect to equiv of Cu^{2+}.

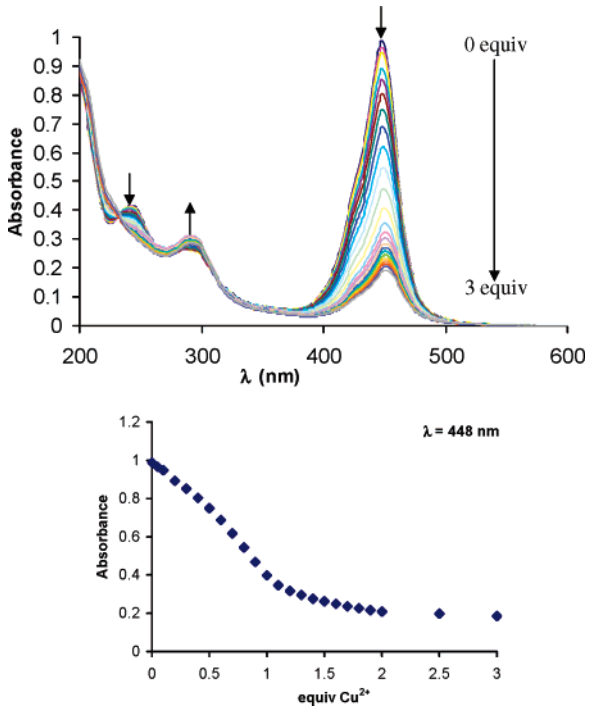

FIGURE 7. UV−vis titration of **17** (10^{-5} M, CH_3CN) in the presence of Cu^{2+} and representation of the variation of absorbance at 448 nm with respect to equiv of Cu^{2+}.

almost complete. Therefore, titration of **14** required the same number of equivalents also needed for the titration of **12** or **13**, and the shape of the representation of the variation of absorbance at 443/447 nm with respect to equiv of Cu^{2+} in Figures 4 and 5 was surprisingly similar, giving indications about a similar mechanism of complexation. This means that compound **14** most probably forms a double pincer complex **14**$[Cu^{2+}]_2$, such as

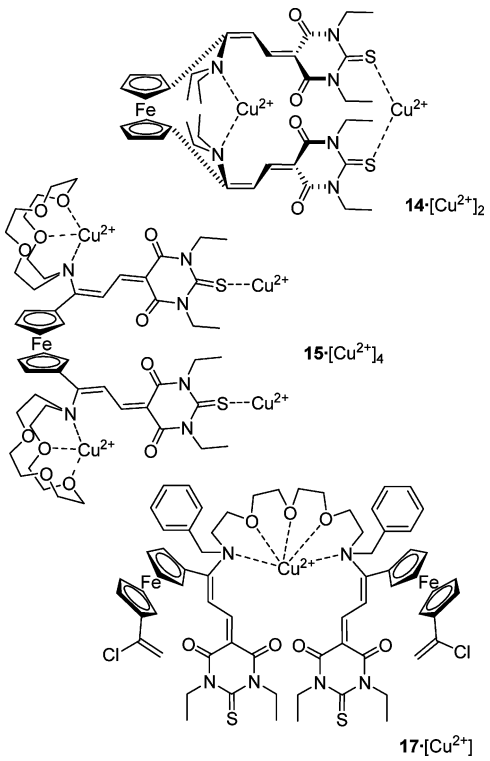

FIGURE 8. Representation of the complexes **14**$[Cu^{2+}]_2$, **15**$[Cu^{2+}]_4$, and **17**$[Cu^{2+}]$ detected by Cu^{2+} titration of ligands **14**, **15**, and **17**.

that represented in Figure 8, thus complexing 1 equiv of Cu^{2+} between the two amino groups and another equivalent between thioxo groups. This behavior was in strong contrast to the behavior shown by UV−vis titration of **15** (10^{-5} M, CH_3CN) in the presence of Cu^{2+} and the representation of the variation of absorbance at 448 nm with respect to equiv of Cu^{2+} shown in Figure 6, in which the presence of isosbestic points similar to the ones observed in previous cases was observed, but also that the extinction of the band at 448 nm was almost completed after the addition of 4 equiv of Cu^{2+}, twice the amount of Cu^{2+} equivalents needed for the titration of **12**−**14**. This behavior is best explained by the gradual formation of a complex **15**$[Cu^{2+}]_4$ such as that represented in Figure 8, in which all Cu^{2+} complexing moieties of **15** acted independently, most probably by steric hindrance of the aza-crown groups.

Determination of complex formation constants was performed on the basis of the data of titration profiles corresponding to compounds **12**−**15** and **17** that were fit using the Origin nonlinear curve-fitting feature according to standard models (see Supporting Information). Because in most titration profiles there are two different regions showing different slopes, corresponding to ML and M_2L complex formation, respectively, data from every region were fit independently (see Figures S6−S14 in the Supporting Information). Titration analysis data gave the stability constants displayed in Table 1 and confirmed the formation in solution of the reported ligand/metal complex stoichiometries. Compounds **12**−**14** showed complexes with 1:2 stoichiometries with related binding constants, and the second binding constant was substantially higher for compound **14**, due to the formation of a pincer complex shown in Figure 8.

The UV−vis titration of **17** (10^{-5} M, CH_3CN) in the presence of Cu^{2+} showed an isosbestic point at 233 nm from 0−2 equiv Cu^{2+} (Figure 11), and the representation of the variation of absorbance at 448 nm with respect to equiv of Cu^{2+} showed a characteristic profile of complexation of 1 equiv Cu^{2+}, which is best fit to a **17**$[Cu^{2+}]$ model (see Figure S15 in the Supporting Information), giving a constant of similar value as the first constant in previous complexes (see Table 1). From this behavior, it was concluded that both amine groups from the polyether moiety in **17** acted cooperatively by complexing 1 equiv of Cu^{2+}, forming a pincer complex that was responsible of the UV−vis variation, and after that, the presence of an additional equiv of Cu^{2+} had little influence on the UV−vis variation. There was no total extinction of the absorbance at 448 nm, thus limiting its use as a copper[II] sensor.

The response of all compounds to the presence of mercury-[II] was certainly intriguing, although less interesting from the point of view of selective sensing, notwithstanding that we performed the titration of the compounds and Hg^{2+} to understand the complexing behavior of the ligands (see Figures S16−S20 in the Supporting Information). UV−vis titration of **12** showed a gradual decrease of the 442 nm signal in the presence of increasing amounts of Hg^{2+} until the absorbance reached a 0.25 value after the addition of 1 equiv of Hg^{2+}. An isosbestic point at 460 nm was visible for all the titration experiments, and another one at 229 nm was visible between 0 and 0.5 equiv of Hg^{2+}. Titration of **13** showed a strong decrease in the 447 nm signal between 0 and 2 equiv of Hg^{2+}; after that, the absorbance reached a constant value of 0.4. It also showed a slow decrease of the 293 nm signal and an increase of the 231 nm signal, and three isosbestic points at 464, 395, and 319 nm were observed for all titration experiments. Titration of **14** showed again a decrease of the 443 nm signal between 0.1 and 1 equiv of Hg^{2+} until the absorbance reached a value of 0.4. Four isosbestic points at 461, 395, 317, and 279 nm were observed for all the titration experiments.

By comparison of the representations obtained for compounds **12** and **14**, it was observed that saturation of the ligand in both cases needed just 1 equiv of Hg^{2+}; therefore, compound **14** formed again a pincer complex between the Hg^{2+} ion, and both substituents bonded to the ferrocene group, an effect that was not observed for the titration of **15** in comparison to **13**. Instead, titration curbs corresponding to **17** showed the formation of a pincer complex with 1 equiv of Hg^{2+}. In all cases, the representation of the variation of absorbance at 442−448 nm with respect to equivalents of Hg^{2+} showed regions with different slopes before the absorbance value was kept constant; therefore, a suitable fitting of the profiles could not be obtained. We then performed the titration of compounds **12**−**15** and

TABLE 1. Complex Formation Constants from Titration Profiles of Compounds 12−15 and 17

complex	log K_1	log K_2	χ^2	R^2
12$[Cu^{2+}]_2$	5.25 ± 0.03	6.53 ± 0.04	$2.4 \times 10^{-4}/5.0 \times 10^{-6}$	0.9911/0.9998
13$[Cu^{2+}]_2$	4.21 ± 0.17	6.50 ± 0.10	$3.0 \times 10^{-5}/2.5 \times 10^{-4}$	0.9989/0.9977
14$[Cu^{2+}]_2$	4.21 ± 0.16	7.23 ± 0.17	$9.1 \times 10^{-6}/1.5 \times 10^{-4}$	0.9993/0.9975
15$[Cu^{2+}]_4$	No adequate model to fit profile			
17$[Cu^{2+}]$	5.71 ± 0.12		1.6×10^{-3}	0.9828

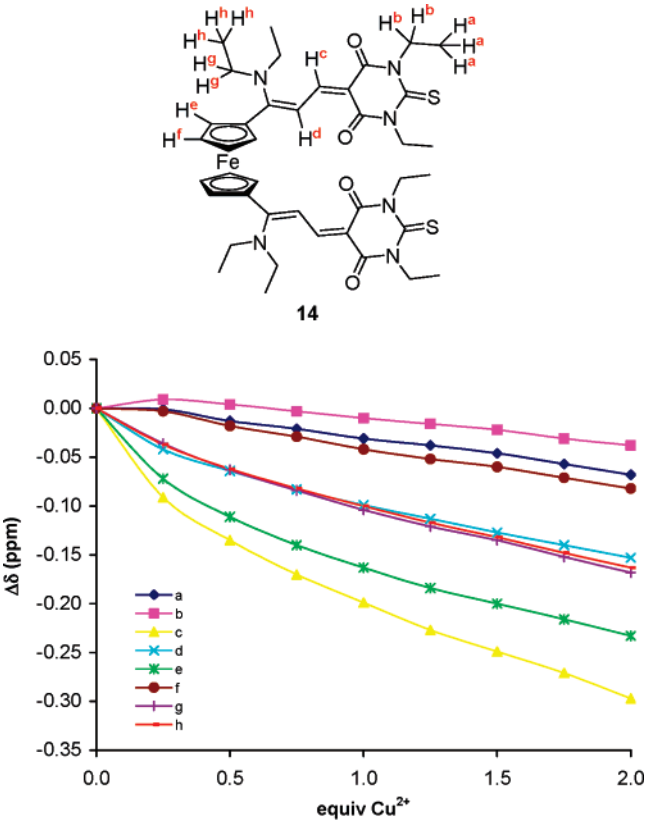

FIGURE 9. Representation of the variation of chemical shifts in ^{1}H NMR corresponding to the protons marked in red of **14** with respect to equiv of Cu^{2+}.

17 in the presence of increasing amounts of Fe^{3+} with the aim of establishing the possible interference of the sensitivity of the ligands with respect to the sensing of Cu^{2+}. Figures S21−S25 in the Supporting Information show the UV−vis titration curbs (10^{-5} M, CH_3CN) in the presence of Fe^{3+} and representations of the variation of the main absorbance signal in every case. The UV−vis titration of compounds **12**−**15** and **17** (10^{-5} M, CH_3CN) in the presence of Fe^{3+} showed almost complete extinction of the main absorption band (442−448 nm) after the addition of several equivalents of Fe^{3+} (4 equiv for **12**, 8 equiv for **13**, 5 equiv for **14**, 11 equiv for **15**, and 5 equiv for **17**). In all cases, the number of equivalents of Fe^{3+} needed for the extinction of the main absorbance band was much larger than the number needed for titration of Cu^{2+}; therefore, the sensitivity of compounds **12**−**15** and **17** to the presence of Fe^{3+} was much lower than for the presence of Cu^{2+}. The titration profiles against equivalents of Fe^{3+} showed regions with different slopes in every case, indicating that different species were formed upon titration of every compound. This fact was confirmed by the absence of isosbestic points in the titration curbs.

We then studied the behavior of compounds **14**−, **15**, and **17** in the presence of increasing amounts of Cu^{2+} by ^{1}H NMR spectroscopy to confirm the interactions shown by UV−vis titration. Therefore, 10^{-3} M solutions of **14**−, **15**, and **17** in $CDCl_3$ were treated with increasing amounts of $Cu(ClO_4)_2$ solutions in CD_3OD, and the ^{1}H NMR spectra were recorded at 20 °C in a 300 MHz NMR machine. The evolution of the main proton shifts for compound **14** is shown in Figure 9. Superimposed figures of selected regions of ^{1}H NMR spectra of **14** that show the detailed evolution of every proton involved in the Cu^{2+} interactions with the ligand are shown in Figures S26−S28 of the Supporting Information.

In general, chemical shift signals of all protons involved in the interactions of **14** and Cu^{2+} are displaced to higher field values, giving lower chemical shifts in the presence of increasing amounts of Cu^{2+}; therefore, a shielding effect is expected after complexation. The effect is more pronounced for the double bond proton **c** than for **d**, for the ferrocene proton **e** than for **f**, and, in a lower extension, for the barbituric ethyl protons **a** than for **b**. Protons g that appeared as a broad signal in the absence of Cu^{2+} were resolved as a quartet after the first addition of 0.25 equiv of Cu^{2+}, indicating that the complexation of Cu^{2+} to the amine nitrogens in **14** fixed the slow rotation of amine ethyl groups. In fact, the effect of complexation in the amine ethyl protons **g** and **h** was similar. The strongest displacements of the chemical shift signals were found for protons **c**, **e**, **g**, and **h**, all of them supporting a complexation of the Cu^{2+} ion by both amino groups that should affect just the protons located in the near vicinity. The fact that protons a were affected more by extension than protons **b** by complexation should be due to interactions between a Cu^{2+} ion and the thione groups, which should affect by more extension to methyl than to methylene groups. All ^{1}H NMR data support the **14**$[Cu^{2+}]_2$ complex shown in Figure 8.

The evolution of the main proton shifts for compound **15** is shown in Figure 10. Superimposed figures of selected regions of ^{1}H NMR spectra of **15**, which show the detailed evolution of every proton involved in the Cu^{2+} interactions with the ligand, are shown in Figures S29−S31 of the Supporting Information.

Except for methylene protons **i**, chemical shift signals of all protons involved in the interactions of **15** and Cu^{2+} are displaced to higher field values, giving lower chemical shifts, in the presence of increasing amounts of Cu^{2+}, a shielding effect of complexation. Again, the effect is more pronounced for the double bond proton **c** than for **d**, for the ferrocene proton **e** than for **f**, and, in a lower extension, for the barbituric ethyl protons **a** than for **b**. The effect of complexation in the aza-crown protons is not very pronounced, although it is more pronounced for the methylene protons **g** near the amine nitrogen than for the rest. The strongest displacements of the chemical shift signals were found for protons **c**, **e**, **g**, and **a**, all of them supporting a complexation of the Cu^{2+} ions by the amino aza-crown groups and the thione groups. All ^{1}H NMR data support the **15**$[Cu^{2+}]_4$ complex shown in Figure 8, although the complexation by the aza-crown oxygen atoms is shown to be much weaker than the complexation exerted by the nitrogen atoms.

The evolution of the main proton shifts for compound **17** is shown in Figure 11. Superimposed figures of selected regions of ^{1}H NMR spectra of **17**, which show the detailed evolution of every proton involved in the Cu^{2+} interactions with the ligand, are shown in Figures S32−S34 of the Supporting Information.

Most chemical shift signals of all protons involved in the interactions of **17** and Cu^{2+} are displaced to higher field values by complexation with Cu^{2+}, but the more flexible structure of **17** gave poorly resolved signals. Again, the effect is more pronounced for the double bond proton **c** than for **d** (ferrocene protons **e** and **f** are not resolved), for the amine methylene protons **g** than for **h** (although there is some effect on **i**), and for the barbituric ethyl protons **a** than for **b**. The effect of complexation in the chlorovinyl protons **j** and **k** was unexpected, being more pronounced for **j**. The strongest displacements of the chemical shift signals were found for protons **a**, **c**, **d**, and

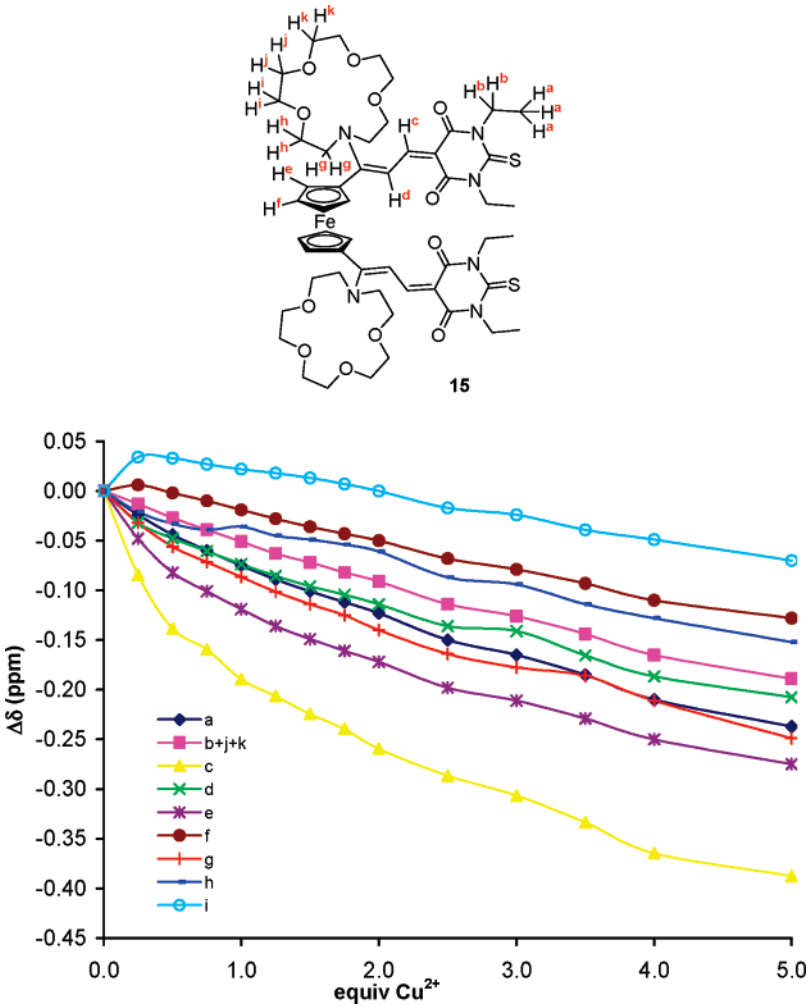

FIGURE 10. Representation of the variation of chemical shifts in ^{1}H NMR corresponding to the protons marked in red of **15** with respect to equiv of Cu^{2+}.

g, all of them supporting a complexation of the Cu^{2+} ions by the amino aza-polyether groups and the thione groups. All ^{1}H NMR data support the **17**$[Cu^{2+}]_2$ complex shown in Figure 8, although the complexation by the polyether oxygen atoms should be weaker than the complexation exerted by the amine nitrogen atoms.

The preference for selective complexation of these compounds and Cu^{2+} is certainly intriguing. According to the Irving and Williams series, if the successive stability constants of complexes of divalent ions of the first transition series are plotted against the atomic number of the element, there is a monotonic increase to a maximum at Cu^{2+} regardless of the nature of the ligand.[32] This order was explained by Irving and Williams[32a,b] as a consequence of the fact that the two parameters, which serve as a guide to the magnitude of the ionic (electrostatic) and covalent interactions (the reciprocal of the metal ionic radius and the sum of the first two ionization energies, respectively), both increase monotonically throughout the series from Mn^{2+} to Cu^{2+} and then decrease from Cu^{2+} to Zn^{2+}. Thus, if water is replaced from $[M(OH_2)_n]^{2+}$ by a ligand of better electron-donating power, the gain in stability will increase with the ionization potential of the metal. The little influence of Zn^{2+} in comparison to Cu^{2+} agrees with the expected behavior. Fe^{3+} binding is probably due to a favorable net entropy of coordination. A large entropy term is common for Fe^{3+} coordination chemistry.[32d] On the other hand, chromogenic sensors based on nitrogen interactions are usually sensitive to both Hg^{2+} and Cu^{2+}.[33] Therefore, a combination of the molecular geometry and complexation trends explain the experimental results.

We then decided to test the sensitivity of these compounds to the presence of the most usual anions as tetrabutylammonium salts in acetonitrile solution. To study the cooperative binding of the two α,α′-groups present in compounds **14**−**15**, we performed a comparative study of the behavior of these compounds in contrast to the corresponding monosubstituted derivatives **12**−**13**. In preliminary experiments, 10^{-5} M solutions in acetonitrile of **12**−**15** and **17** decolorized partially in the presence of 5 equiv of F^-, CN^-, BzO^-, AcO^-, and $H_2PO_4^-$ as Bu_4N^+ salts in acetonitrile, all compounds being unchanged by the presence of 5 equiv of each one of the other anions studied. As a representative example, Figure 12 shows the effect of the

(32) (a) Irving, H.; Williams, R. J. P. *Nature* **1948**, *162*, 746−747. (b) Irving, H.; Williams, R. J. P. *J. Chem. Soc.* **1953**, 3192−3210. Recent examples: (c) Gorelsky, S. I.; Basumallick, L.; Vura-Weis, J.; Sarangi, R.; Hodgson, K. O.; Hedman, B.; Fujisawa, K.; Solomon, E. I. *Inorg. Chem.* **2005**, *44*, 4947−4960. (d) Grossoehme, N. E.; Akilesh, S.; Guerinot, M. L.; Wilcox, D. E. *Inorg. Chem.* **2006**, *45*, 8500−8508.

(33) See, for example: Lee, H. G.; Lee, J.-E.; Choi, K. S. *Inorg. Chem. Commun.* **2006**, *9*, 582−585 and references therein.

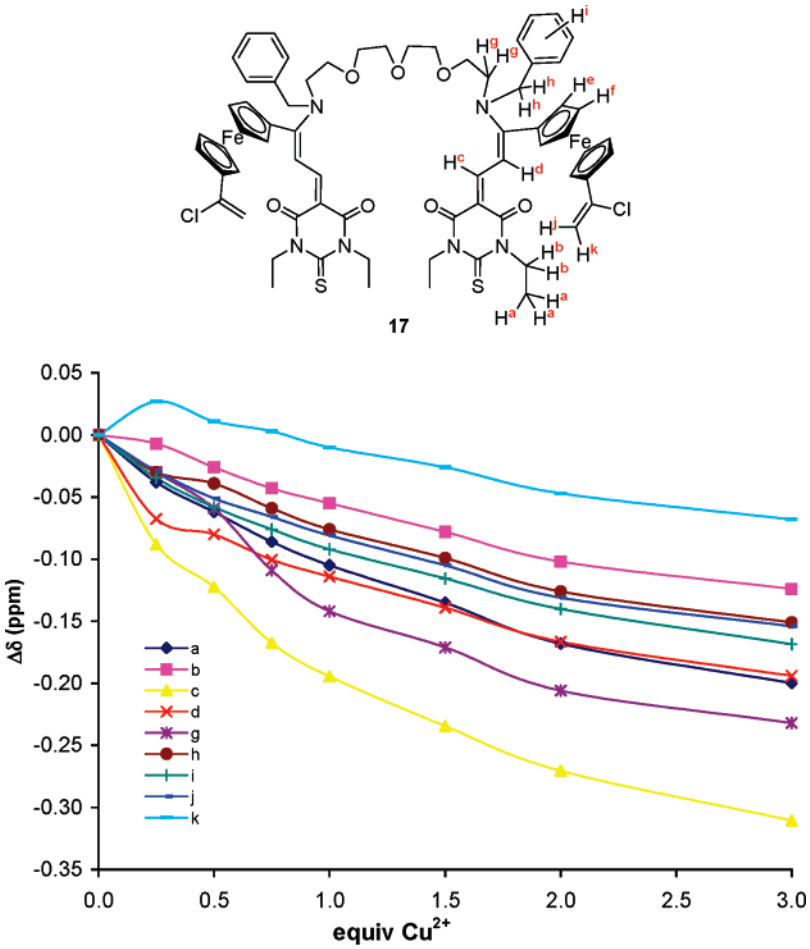

FIGURE 11. Representation of the variation of chemical shifts in ^{1}H NMR corresponding to the protons marked in red of **17** with respect to equiv of Cu^{2+}.

FIGURE 12. Effect of the addition of 5 equiv of every indicated anion to a 10^{-5} M solution of **12** in acetonitrile.

addition of 5 equiv of every indicated anion to a 10^{-5} M solution of **12** in acetonitrile. The effect was similar for all compounds, independent of the structural variations of every compound, but the naked-eye detection of the anions was much less evident than in the case of the previously studied Cu^{2+} cation.

The changes are more evident by UV−vis spectroscopy. The UV−vis spectrum of compound **12** in the presence of 5 equiv of every anion in acetonitrile showed attenuation of the 442 nm band in the presence of F^-, CN^-, BzO^-, and AcO^-, some less pronounced attenuation in the presence of $H_2PO_4^-$, and the simultaneous occurrence of a new absorption band centered at 370 nm (Figure 13). The effect of the addition of 5 equiv of every anion in the UV−vis spectrum of a solution of every one of the compounds was similar; therefore, the complexation mechanism did not seem to depend on the presence of a special feature of every compound but was due to the common structure of all studied compounds.

We then performed accurate titrations of 10^{-5} M solutions in acetonitrile of every compound by the addition of increasing amounts of concentrated acetonitrile solutions of tetrabutylammonium salts of every active anion, taking the UV−vis spectrum of all additions and representing the variation of the maximum wave absorption with respect to the number of added equivalents of every studied anion. As representative examples, Figures 14−16 show the UV−vis titration of **12** (10^{-5} M, CH_3CN) in the presence of the most active anions CN^-, AcO^-, and BzO^-. The corresponding UV−vis titration curbs obtained for **13**−**15** and **17** in the presence of the most active anions were similar.

In all cases, the gradual attenuation of the 442 nm band and the appearance of the 367 nm band, which increased significantly after the addition of the first equiv of anion, were observed. The presence of two isosbestic points at 405 and 464 nm, after the addition of the first equivalent of anion, was detected. To compare the effect of the addition of every anion

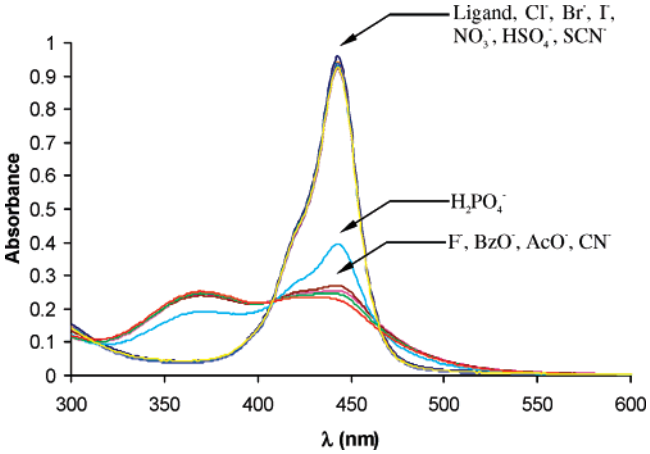

FIGURE 13. UV−vis spectrum of **12** (10^{-5} M, CH_3CN) in the presence of 5 equiv of every anion.

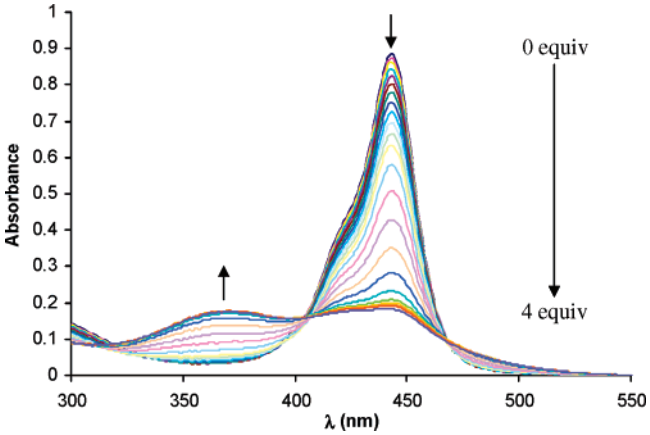

FIGURE 14. UV−vis titration of **12** (10^{-5} M, CH_3CN) in the presence of CN^-.

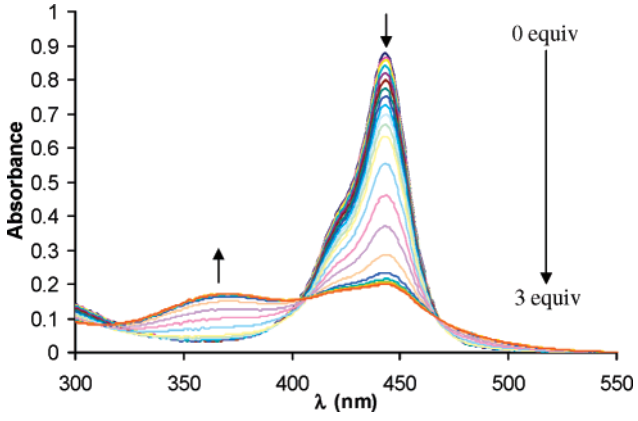

FIGURE 15. UV−vis titration of **12** (10^{-5} M, CH_3CN) in the presence of AcO^-.

studied, we represented the variation of absorbance of a solution of every compound (10^{-5} M, CH_3CN) at 442−448 nm with respect to equivalents of F^-, CN^-, AcO^-, BzO^-, and $H_2PO_4^-$ until the absorbance of the main UV−vis signal became constant. The corresponding titration profiles are shown in Figures 17−21.

In all cases studied, the behavior of fluoride and dihydrogen phosphate anions appeared to be different from the rest of the anions, giving titration curbs with sections having different

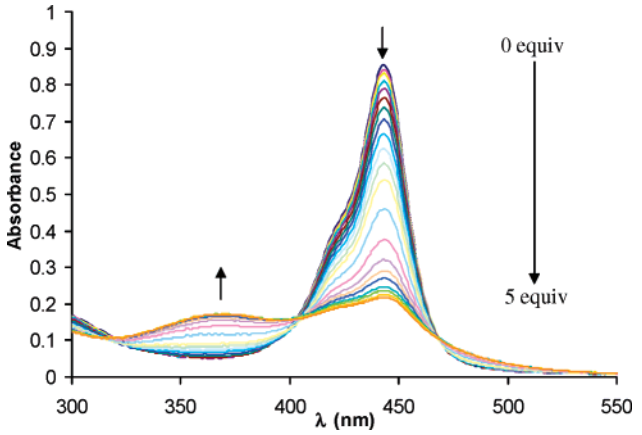

FIGURE 16. UV−vis titration of **12** (10^{-5} M, CH_3CN) in the presence of BzO^-.

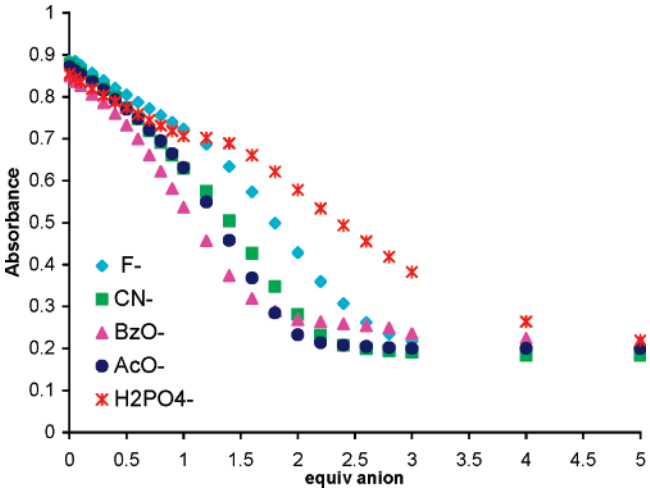

FIGURE 17. Representation of the variation of absorbance of **12** at 442 nm with respect to equiv of F^-, CN^-, AcO^-, BzO^-, and $H_2PO_4^-$.

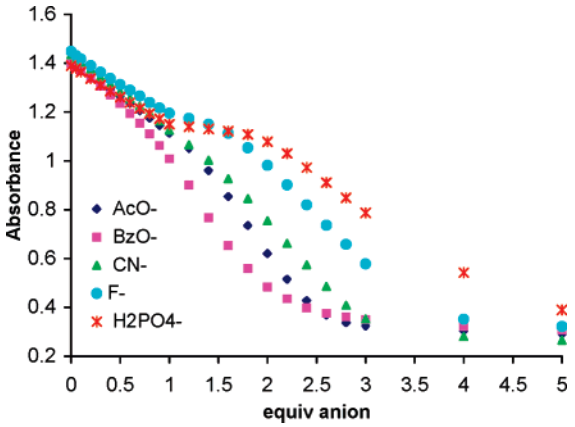

FIGURE 18. Representation of the variation of absorbance of **13** at 447 nm with respect to equiv of F^-, CN^-, AcO^-, BzO^-, and $H_2PO_4^-$.

slopes, typically between 0 and 1 equiv and 1− and 6 equiv of anion, and saturation of the band at a higher number of equivalents of anion, typically 3−4 equivalents or even more. Therefore, the compounds showed less sensitivity to these two anions. All compounds showed comparable sensitivity to the rest of the anions, benzoate, acetate, and cyanide, the absorbance of the main band becoming constant at around 2 equiv of anion.

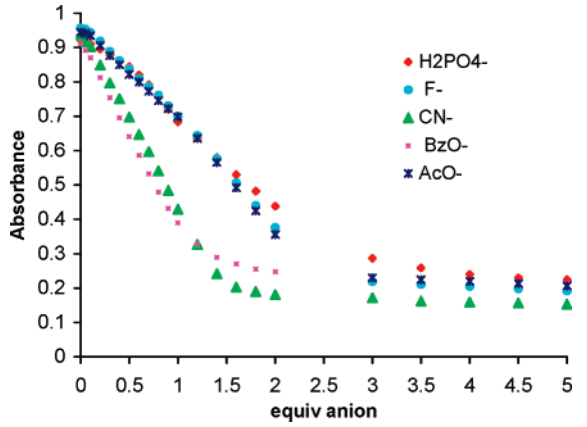

FIGURE 19. Representation of the variation of absorbance of **14** at 443 nm with respect to equiv of F^-, CN^-, AcO^-, BzO^-, and $H_2PO_4^-$.

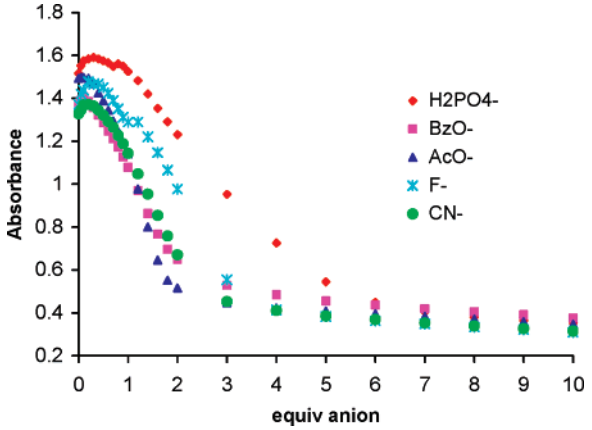

FIGURE 20. Representation of the variation of absorbance of **15** at 443 nm with respect to equiv of F^-, CN^-, AcO^-, BzO^-, and $H_2PO_4^-$.

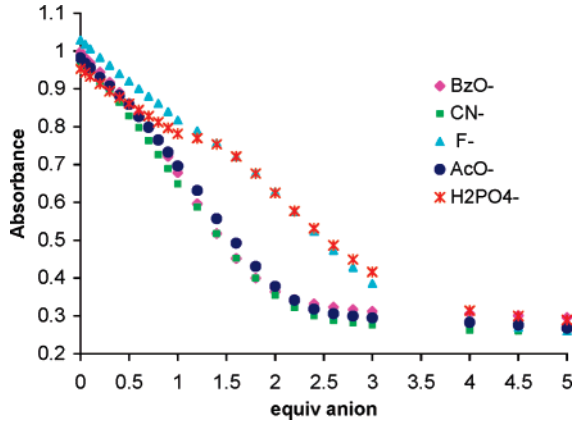

FIGURE 21. Representation of the variation of absorbance of **17** at 443 nm with respect to equiv of F^-, CN^-, AcO^-, BzO^-, and $H_2PO_4^-$.

The only exception was compound **14** (Figure 19) that showed an increased sensitivity for the benzoate and cyanide anions over the acetate anion. In fact, **14** needed twice the equivalents of acetate in comparison to the equivalents of benzoate needed to arrive to a constant minimum value of absorbance of the 443 nm band. The most striking fact was that all compounds, whether they had one or two signaling groups, needed a comparable number of equivalents of every anion to arrive at a minimum absorbance value of the main absorbance band. This fact can be explained by a cooperative action of both signaling units in the interaction with every anion. In fact, the most effective interactions were noticed for compound **14** and benzoate, a planar anion, or for cyanide, whose interaction decreased the absorbance of the band to the minimum value.

TABLE 2. Binding Constants from Titration Profiles of Compounds 12−15 and 17

sensor	anion	log K_1	log K_2	χ^2	R^2
14	benzoate	4.11 ± 0.17	5.98 ± 0.16	6.0×10^{-5}	0.9991
14	cyanide	4.59 ± 0.10	5.41 ± 0.08	4.1×10^{-4}	0.9959
15	benzoate	3.93 ± 0.23	6.01 ± 0.22	5.7×10^{-4}	0.9965
15	Acetate	4.08 ± 0.15	6.05 ± 0.12	4.5×10^{-3}	0.9812
15	Cyanide	2.23 ± 0.05	7.67 ± 0.05	8.6×10^{-4}	0.9959
17	benzoate	4.62 ± 0.03	4.93 ± 0.02	1.0×10^{-4}	0.9988

Determination of selected binding constants was performed on the basis of data of titration profiles corresponding to compounds **12−15** and **17** that were fit using the Origin nonlinear curve-fitting feature according to the standard models (see Supporting Information). Most titration profiles were not suitable for an appropriate fitting because they did not adapt to the model or just for the lack of a suitable model, but in selected cases, the best fitting was obtained (see Figures S6−S14 in the Supporting Information). Titration analysis data gave the binding constants displayed in Table 2 and confirmed the formation in solution of the reported ligand/anion complex stoichiometries. Compounds **14−15**, and **17** showed anion interactions having 1:2 stoichiometries with related binding constants in several cases, and the second binding constant was substantially higher for compound **15** and cyanide, probably due to higher stabilization of the intermediate by the presence of the crown ether moieties.

To understand the interaction of these compounds and anions, we performed accurate titrations of compound **14** in the presence of increasing amounts of CN^- by ^1H NMR spectroscopy to complement the information shown by UV−vis titration. Therefore, a 7×10^{-3} M solution of **14** in $CDCl_3$ was treated with increasing amounts of $Bu_4N^+CN^-$ solutions in $CDCl_3$, and the ^1H NMR spectra were recorded at 20 °C in a 300 MHz NMR machine. Superimposed figures of the δ 3−10 ppm region of the ^1H NMR spectrum of **14**, which show a detailed evolution of every proton involved in the CN^- interactions with the ligand, after addition of 0−2 equiv of anion, are shown in Figure 22. In the ^1H NMR spectra, it is observed that the signal corresponding to proton **c** splits into two equivalent signals after the addition of 1.50 equiv of cyanide anion, one of the signals coincided with the original, and the other one was displaced upfield δ −0.63. The signal of the vicinal proton **d** also split into two very close signals with very little displacement of the second one (δ −0.03). The signal of protons **b** also split into two multiplets, one of them displaced downfield δ 0.25 and composed of two partially superimposed unresolved quadruplets. The integral of the new group of signals and the original one was almost similar after the addition of 1.50 equiv of cyanide anion. Partial loss of symmetry of the signals corresponding to protons **e** and **f** was also observed. The presence of water in the titration experiments was due to water of crystallization from the salts, as was also evidenced in Figures S27, S30, and S33 in the Supporting Information. Water plays important roles in the complexation.[34] In this study, high amounts of water exert

(34) See, for example: Bonar-Law, R. P.; Sanders, J. K. M. *J. Am. Chem. Soc.* **1995**, *117*, 259−271.

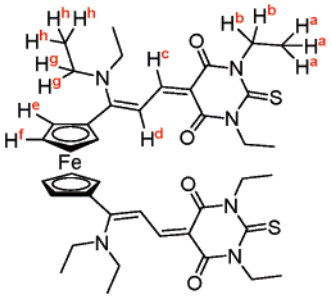

14

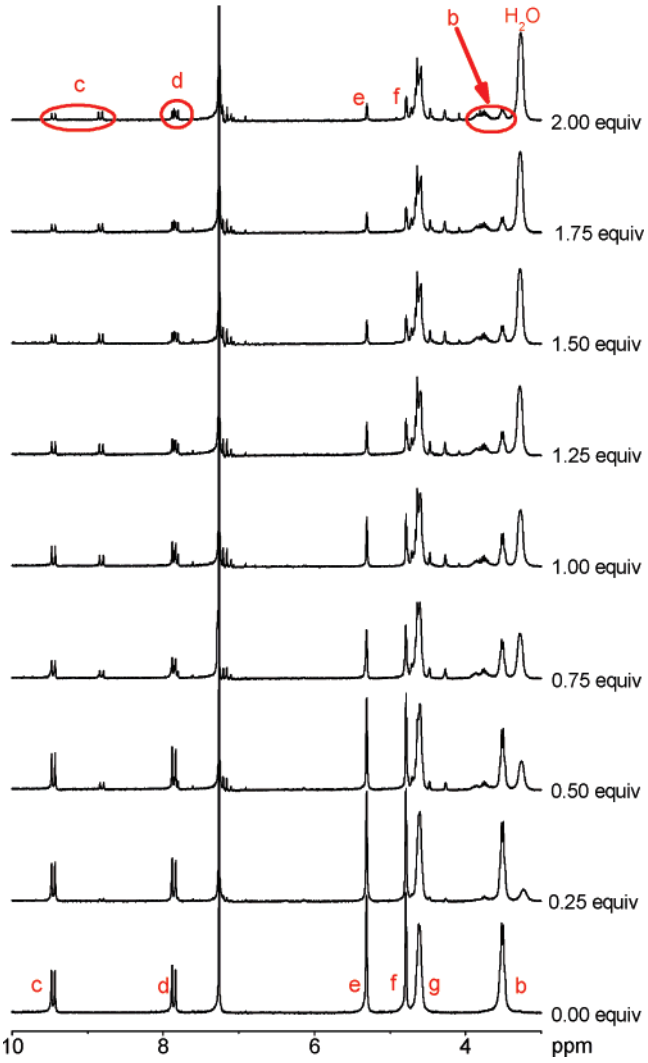

FIGURE 22. Evolution of the δ 3−10 ^{1}H NMR region of **14** ($CDCl_3$, 300 MHz, 7 mM, 20 °C) after addition of 0−2 equiv of $Bu_4N^+CN^-$ ($CDCl_3$).

a detrimental effect on the solubility of the ligand, therefore interfering with the measurements, but low amounts of water (a few equivalents included as the crystallization water of the salts) do not apparently affect the binding ability of the ligands with the species studied.

From the ^{1}H NMR titration, it can be concluded that simultaneous interaction of the anion with the β-position of the thiobarbituric carbonyl (a reversible 1,4-addition) and with the thiobarbituric carbonyl group (a reversible 1,2-addition) in addition to a restricted rotation of the ferrocene group after the

SCHEME 9

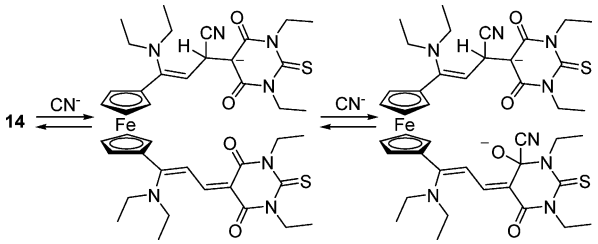

reversible additions could explain the evolution of the ^{1}H NMR spectra (Scheme 9).

For comparison to the latter, we performed the titration of compound **17** in the presence of increasing amounts of CN^- by ^{1}H NMR spectroscopy in the same conditions employed previously. Superimposed figures of the δ 5−10 ppm region of the ^{1}H NMR spectrum of **17**, which show a detailed evolution of the main protons involved in the CN^- interactions with the ligand, after the addition of 0−3 equiv of anion, are shown in Figure S35 in the Supporting Information. The ^{1}H NMR spectra showed that the signal corresponding to vinylic proton **c** split into two nonequivalent signals during titration with increasing amounts of cyanide anion and that one of the signals displaced upfield δ −0.92 until extinction of the original signal at high concentrations of cyanide anion. The signal of the vicinal proton **d** also split into two very close signals with displacement of the second one upfield δ −0.20 with gradual extinction of the original signal. The signals of chlorovinyl protons **j** and **k** are also affected after the addition of 2 equiv of cyanide anion, indicating that the interactions with anions have implications on the free rotation of the ferrocene units. All these experiments support the reversible 1,2- and 1,4-addition of anions to the unsaturated chain of ferrocene derivatives, thus interrupting coordination and giving rise to a decrease in the main absorption band and the appearance of a new absorption band at shorter wavelengths. In all cases, the interactions of the different anions with the sensing units were less effective than in the case of interactions of copper[II] that conducted the total extinction of the main absorption band. In the case of anion detection, even the most sensitive compound **14** and benzoate or cyanide anions conducted a decrease of the main absorption band to a residual value of 0.2. This fact permitted the naked-eye detection of the copper[II] cation without risk of interaction of the most common anions but, at the same time, permitted the anion sensing of benzoate, acetate, or cyanide in the presence of other types of common cations. The cooperative binding of both α,α′-substituents of the ferrocene derivative **14** to the detected cation and anions was remarkable.

In conclusion, we have reported several new ferrocene derivatives bearing two donor−acceptor systems in which the ferrocene unit acts both as a donor group and as a rotating spacer. These molecules are capable of selectively sensing copper[II] and benzoate, acetate, or cyanide anions by cooperative binding of the two α,α′-groups bonded to the ferrocene nucleus. The reported ferrocene sensors permit the naked-eye selective colorimetric detection of copper[II] cation and, less effectively, of benzoate, acetate, or cyanide anions, all ions of special toxicological and biological relevance.

Experimental Section

1-(1-Chloro-2-formylvinyl)-1′-(1-chlorovinyl)ferrocene 2 and 1,1′-Bis(1-chloro-2-formylvinyl)ferrocene[29a] 3. Phosphoryl trichloride ($POCl_3$, 0.8 mL, ρ = 1.645 g/mL, 8.33 mmol) was dissolved

in DMF (3 mL) at 0 °C under nitrogen atmosphere, and the mixture was stirred at 0 °C for 1 h, then 1,1′-diacetylferrocene[30] (375 mg, 1.39 mmol) in DMF (3 mL) was added dropwise for 15 min, and the resulting mixture was stirred for 2 h at 0 °C and additionally stirred for 1 h at room temperature. Then, the mixture was poured on a solution of sodium acetate (AcONa, 20% w/v in H_2O, 50 mL), stirred at room temperature for 1.5 h, and extracted with CH_2Cl_2 (3 × 50 mL). The combined extracts were washed with H_2O, dried with $MgSO_4$, and evaporated under reduced pressure. The residue was subjected to chromatography (3 × 20 cm, silica, CH_2Cl_2/hexane 1:1 to CH_2Cl_2) to obtain **2** as a purple−red solid [CH_2Cl_2/hexane, 278 mg, 60%, ^{1}H NMR (200 MHz, $CDCl_3$) δ 10.10 (d, 1H, J = 6.8 Hz), 6.34 (d, 1H, J = 6.8 Hz), 5.40 (s, 1H), 5.33 (s, 1H), 4.72−4.34 (m, 8H)] and **3** as a purple solid [CH_2Cl_2/hexane, 120 mg, 24%, ^{1}H NMR (200 MHz, $CDCl_3$) δ 10.07 (d, 2H, J = 7.0 Hz), 6.34 (d, 2H, J = 7.0 Hz), 4.77 (s, 4H), 4.60 (s, 4H)] that agreed with the reported compounds.

(*Z*)-1-(1-Chloro-4,4-dicyano-1,3-butadienyl)-1′-(1-chlorovinyl)-ferrocene 4. Malononitrile (370 mg, 5.60 mmol) and DABCO (221 mg, 1.98 mmol) were added to a solution of compound **2** (300 mg, 0.90 mmol) in CH_2Cl_2 (20 mL), and the mixture was stirred for 10 min, then poured on water (50 mL), and extracted with CH_2Cl_2 (3 × 50 mL). The combined organic extracts were washed with H_2O and dried ($MgSO_4$), and the solvent was evaporated under reduced pressure. The residue was subjected to column chromatography (3 × 20 cm, silica, CH_2Cl_2/hexane 1:1) to give **4** (258 mg, 75%) as a deep-blue solid (CH_2Cl_2/hexane), mp 86−87 °C; ^{1}H NMR (300 MHz, $CDCl_3$) δ 7.92 (d, 1H, J = 11.5 Hz), 6.84 (d, 1H, J = 11.5 Hz), 5.40 (s, 1H), 5.34 (s, 1H), 4.82 (s, 2H), 4.72 (s, 2H), 4.56 (s, 2H), 4.35 (s, 2H); ^{13}C NMR (75 MHz, $CDCl_3$) δ 154.1, 152.9, 136.0, 115.8, 114.4, 112.4, 110.6, 86.2, 81.3, 80.1, 75.0, 72.2, 70.9, 69.8; IR (KBr) $\tilde{\nu}$ 3037, 2919, 2848, 2233 (CN), 1665, 1562, 1444, 1276, 1229, 1199, 482 cm^{-1}; EIMS *m*/*z* (%): 386 (M^+ + 4, 11), 384 (M^+ + 2, 83), 382 (M^+, 100), 323 (25), 322 (46), 260 (55), 90 (39). Anal. Calcd for $C_{18}H_{12}Cl_2FeN_2$: C, 56.44; H, 3.16; N, 7.31. Found: C, 56.25; H, 3.04; N, 7.19.

(*Z*),(*Z*)-1,1′-Bis(1-chloro-4,4-dicyano-1,3-butadienyl)ferrocene 5. Malononitrile (33 mg, 0.494 mmol) and DABCO (18 mg, 0.165 mmol) were added to a solution of compound **3** (30 mg, 0.082 mmol) in CH_2Cl_2 (3 mL), and the mixture was stirred for 15 min, then poured on an aqueous solution of HCl (1 M, 50 mL) and extracted with CH_2Cl_2 (2 × 30 mL). The combined organic extracts were washed with H_2O and dried ($MgSO_4$), and the solvent was evaporated under reduced pressure. The residue was subjected to column chromatography (3 × 15 cm, silica, CH_2Cl_2/hexane 1:1 to CH_2Cl_2) to give **5** (30 mg, 79%) as a deep-blue solid (CH_2Cl_2/hexane), mp 243−244 °C; ^{1}H NMR (200 MHz, $CDCl_3$) δ 7.88 (d, 2H, J= 11.7 Hz), 6.86 (d, 2H, J = 11.7 Hz), 4.86 (s, 4H), 4.73 (s, 4H); ^{13}C NMR (50 MHz, $CDCl_3$) δ 153.7, 151.2, 116.8, 113.8, 112.2, 82.8, 82.6, 75.9, 71.7; IR (KBr) $\tilde{\nu}$ 3094, 3047, 2924, 2233 (CN), 1583, 1557, 1444, 1337, 1276, 1230, 1204, 1040, 856, 502 cm^{-1}; APCIMS *m*/*z* 461 (M^+ + 2, 63), 459 (M^+, 100), 325 (32), 289 (58), 260 (32), 183 (30), 149 (41). Anal. Calcd for $C_{22}H_{12}Cl_2FeN_4$: C, 57.55; H, 2.63; N, 12.20. Found: C, 57.38; H, 2.44; N, 12.09.

(*Z*)-5-{3-[1′-(1-Chlorovinyl)ferrocen-1-yl]-3-chloroallylidene}-1,3-diethyl-2-thioxodihydropyrimidine-4,6(1*H*,5*H*)-dione 6. 1,3-Diethyl-2-thiobarbituric acid (271 mg, 1.356 mmol) and DABCO (152 mg, 1.356 mmol) were added to a solution of compound **2** (151 mg, 0.452 mmol) in CH_2Cl_2 (10 mL), and the mixture was stirred at room temperature for 5 min, then poured on an aqueous solution of HCl (1 M, 10 mL) and extracted with CH_2Cl_2 (2 × 30 mL). The combined organic extracts washed with H_2O and dried ($MgSO_4$), and the solvent was evaporated under reduced pressure. The residue was subjected to column chromatography (3 × 15 cm, silica, CH_2Cl_2/hexane 1:1) to give **6** (185 mg,79%) as a green solid (CH_2Cl_2/hexane), mp 101−102 °C; ^{1}H NMR (300 MHz, $CDCl_3$) δ 8.60 (d, 1H, J = 12.1 Hz), 8.36 (d, 1H, J = 12.1 Hz), 5.38 (s, 1H), 5.29 (s, 1H), 4.93 (s, 2H), 4.73 (s, 2H), 4.55 (m, 6H), 4.35 (s, 2H), 1.30 (m, 6H); ^{13}C NMR (75 MHz, $CDCl_3$) δ 178.7, 160.8, 159.9, 157.3, 151.2, 136.1, 119.1, 113.3, 110.5, 86.3, 82.9, 75.3, 72.6, 71.3, 69.9, 43.8, 43.2, 12.5, 12.4; IR (KBr) $\tilde{\nu}$ 3083, 2976, 2930, 1675 (C═O), 1542, 1445, 1383, 1240, 1117 (C═S), 892, 830, 733, 487 cm^{-1}; APCIMS *m*/*z* 519 (M^+ + 2, 25), 517 (M^+ + 1, 34), 481 (M^+ − HCl, 8), 391 (4), 302 (65), 280 (100), 264 (91), 197 (15). Anal. Calcd for $C_{23}H_{22}Cl_2FeN_2O_2S$: C, 53.41; H, 4.29; N, 5.42. Found: C, 53.29; H, 4.17; N, 5.28.

(*Z*),(*Z*)-1,1′-Bis[1-chloro-3-(1,3-diethyl-2-thioxo-4,6(1*H*,5*H*)-dioxodihydropyrimidine-5-ylidene)allyl]ferrocene 7. 1,3-Diethyl-2-thiobarbituric acid (165 mg, 0.824 mmol) and DABCO (46 mg, 0.412 mmol) in CH_2Cl_2 (2 mL) were added to a solution of compound **3** (50 mg, 0.137 mmol) in CH_2Cl_2 (3 mL), and the mixture was stirred at room temperature for 5 min, then poured on an aqueous solution of HCl (1 M, 50 mL), and extracted with CH_2Cl_2 (2 × 30 mL). The combined organic extracts were washed with H_2O and dried ($MgSO_4$), and the solvent was evaporated under reduced pressure. The residue was subjected to column chromatography (3 × 20 cm, silica, CH_2Cl_2) to give **7** (95 mg, 95%) as a green solid (CH_2Cl_2/hexane), mp >250 °C; ^{1}H NMR (400 MHz, $CDCl_3$) δ 8.39 (d, 2H, J = 12.2 Hz), 8.10 (d, 2H, J = 12.2 Hz), 4.96 (s, 4H), 4.67 (s, 4H), 4.47 (m, 8H), 1.26 (m, 12H); ^{13}C NMR (100 MHz, $CDCl_3$) δ 178.5, 160.5, 159.6, 153.4, 150.8, 119.4, 114.3, 84.7, 75.2, 72.1, 43.8, 43.2, 12.4, 12.3; IR (KBr) $\tilde{\nu}$ 3109, 2975, 2914, 2848, 1670 (C═O), 1552, 1527, 1445, 1388, 1280, 1230, 1199, 1112 (C═S), 467 cm^{-1}; APCIMS *m*/*z* 727 (M^+ + 1, 1), 691 (M^+ − Cl, 100), 391 (21), 301 (53), 273 (31), 186 (19). Anal. Calcd for $C_{32}H_{32}Cl_2FeN_4O_4S_2$: C, 52.83; H, 4.43; N, 7.70. Found: C, 52.68; H, 4.28; N, 7.58.

(*Z*)-1-(1-Dimethylamino-4,4-dicyano-1,3-butadienyl)-1′-(1-chlorovinyl)ferrocene 8. Na_2CO_3 (112 mg, 1.040 mmol) and diethylamine (0.01 mL, 0.105 mmol) were added to a solution of compound **4** (20 mg, 0.052 mmol) in CH_2Cl_2 (3 mL), and the mixture was stirred at room temperature for 18 h and then filtered, and the solvent was evaporated under reduced pressure. The residue was subjected to column chromatography (3 × 20 cm, silica, cyclohexane/CH_2Cl_2 1:1 to CH_2Cl_2) to give **8** (15 mg, 68%) as an orange solid (CH_2Cl_2/hexane), mp 149−150 °C; ^{1}H NMR (400 MHz, $CDCl_3$, two rotamers were detected) δ 8.97 (br s, 0.5H), 7.51 (d, 0.5H, J = 12.8 Hz), 5.83 (d, 0.5H, J = 12.8 Hz), 5.65 (d, 0.5H, J = 13.2 Hz), 5.50 (dd, 1H, J_1 = 12.0 Hz, J_2 = 1.6 Hz), 5.32 (dd, 1H, J_1 = 12.0 Hz, J_2 = 1.6 Hz), 4.77 (t, 1H, J = 2.0 Hz), 4.60 (t, 1H, J = 2.0 Hz), 4.56 (t, 1H, J = 2.0 Hz), 4.53 (m, 2H), 4.43 (dt, 2H, J_1 = 6.4 Hz, J_2 = 2.0 Hz), 4.37 (t, 1H, J = 2.0 Hz), 3.52 (m, 2H), 3.35 (br s, 2H), 1.25 (m, 6H); ^{13}C NMR (100 MHz, $CDCl_3$, two rotamers were detected) δ 169.6, 164.6, 157.3, 151.8, 137.4, 136.9, 118.7, 118.6, 116.1, 111.3, 110.5, 100.8, 96.9, 85.4, 84.7, 79.8, 73.8, 73.1, 73.0, 72.5, 72.1, 69.6, 69.5, 60.6, 59.6, 51.3, 46.0, 43.1, 29.7, 26.9, 14.8, 11.7; IR (KBr) $\tilde{\nu}$ 2919, 2202 (CN), 1603, 1552, 1470, 1424, 1260 cm^{-1}; APCIMS *m*/*z* 422 (M^+ + 3, 15), 421 (M^+ + 2, 11), 420 (M^+ + 1, 49), 360 (28), 329 (22), 326 (100), 312 (40), 149 (14). Anal. Calcd for $C_{22}H_{22}ClFeN_3$: C, 62.95; H, 5.28; N, 10.01. Found: C, 62.83; H, 5.12; N, 9.88.

(*Z*)-1-[1-(1,4,7,10-Tetraoxa-13-azacyclopentadec-13-yl)-4,4-dicyano-1,3-butadienyl]-1′-(1-chlorovinyl)ferrocene 9. Na_2CO_3 (10 mg, 0.088 mmol) and 1,4,7,13-tetraoxa-10-azacyclopentadecane (12 mg, 0.055 mmol) were added to a solution of compound **4** (10 mg, 0.026 mmol) in CH_2Cl_2 (2 mL), and the mixture was stirred at room temperature for 24 h and then filtered, and the solvent was evaporated under reduced pressure. The residue was subjected to flash column chromatography (3 × 10 cm, silica, CH_2Cl_2/AcOEt 9:1) to give **9** (10 mg, 67%) as an orange solid (CH_2Cl_2/AcOEt), mp 141−143 °C; ^{1}H NMR (400 MHz, $CDCl_3$) δ 8.96 (br s, 1H), 5.90 (br s, 1H), 5.52 (s, 1H), 5.34 (s, 1H), 4.56 (s, 4H), 4.46 (s, 2H), 4.37 (s, 2H), 3.73 (m, 20H); ^{13}C NMR (100 MHz, $CDCl_3$) δ 169.1, 168.5, 165.5, 157.6, 136.9, 118.4, 115.8, 111.2, 101.6, 99.9, 85.4, 74.1, 72.6, 72.4, 71.1, 70.5, 70.1, 69.6, 53.7, 53.6; IR (KBr) $\tilde{\nu}$ 2925, 2852, 2208 (CN), 1619, 1552, 1516, 1460, 1352,

1250, 1116 cm^{-1}; APCIMS *m/z* 568 ($M^+ + 3$, 34), 567 ($M^+ + 2$, 32), 566 ($M^+ + 1$, 100), 476 (25), 440 (24). Anal. Calcd for $C_{28}H_{32}ClFeN_3O_4$: C, 59.43; H, 5.70; N, 7.43. Found: C, 59.29; H, 5.60; N, 7.32.

(*Z*),(*Z*)-1,1′-Bis(1-dimethylamino-4,4-dicyano-1,3-butadienyl)-ferrocene 10. Na_2CO_3 (82 mg, 0.773 mmol) and diethylamine (0.025 mL, 0.246 mmol) were added to a solution of compound **5** (24 mg, 0.052 mmol) in CH_2Cl_2 (3 mL), and the mixture was stirred at room temperature for 18 h and then filtered, and the solvent was evaporated under reduced pressure. The residue was subjected to flash column chromatography (3 × 15 cm, silica, CH_2Cl_2/MeOH 9:1) to give **10** (27 mg, 96%) as an orange solid (CH_2Cl_2), mp 90−91 °C; ^{1}H NMR (400 MHz, $CDCl_3$, several rotamers were detected) δ 9.31 (m, 1H), 7.63 (d, 0.5H, J = 12.6 Hz), 7.32 (d, 0.5H, J = 12.6 Hz), 5.84 (m, 1H), 5.67 (d, 1H, J = 12.6 Hz), 4.92 (m, 1H), 4.73−4.58 (m, 7H), 3.48−3.32 (m, 8H), 1.25 (m, 12H); ^{13}C NMR (100 MHz, $CDCl_3$, several rotamers were detected) δ 155.7, 152.7, 152.3, 119.1−118.4 (unresolved signals), 116.1, 115.5, 100.5, 98.1, 97.0, 85.2, 81.0, 75.7, 74.5, 73.6, 73.3, 73.0, 71.9, 71.5, 71.0, 51.6, 47.4, 43.5, 29.6, 14.4, 11.8; IR (KBr) $\tilde{\nu}$ 2930, 2197 (CN), 1608, 1562, 1521, 1470, 1419, 1342, 1260 cm^{-1}; APCIMS *m/z* 534 ($M^+ + 2$, 34), 533 ($M^+ + 1$, 100), 326 (16), 312 (10), 149 (9). Anal. Calcd for $C_{30}H_{32}FeN_6$: C, 67.67; H, 6.06; N, 15.78. Found: C, 67.49; H, 5.90; N, 15.65.

(*Z*),(*Z*)-1,1′-Bis[1-(1,4,7,10-tetraoxa-13-azacyclopentadec-13-yl)-4,4-dicyano-1,3-butadienyl]ferrocene 11. Na_2CO_3 (106 mg, 1.018 mmol) and 1,4,7,13-tetraoxa-10-azacyclopentadecane (77 mg, 0.353 mmol) in CH_2Cl_2 (2 mL) were added to a solution of compound **5** (26 mg, 0.057 mmol) in CH_2Cl_2 (10 mL), and the mixture was stirred under reflux for 24 h and stirred for an additional 24 h at room temperature and then filtered, and the solvent was evaporated under reduced pressure. The residue was subjected to flash column chromatography (3 × 15 cm, silica, CH_2Cl_2 to CH_2Cl_2/MeOH 5:1) to give **11** (28 mg, 60%) as an orange solid (CH_2Cl_2), mp 73−74 °C; ^{1}H NMR (300 MHz, $CDCl_3$) δ 9.25 (br s, 1.5H), 7.43 (d, 0.5H, J = 12.6 Hz), 6.08 (d, 2H, J = 12.6 Hz), 4.67 (s, 4H), 4.58 (s, 4H), 3.73−3.58 (m, 40H); ^{13}C NMR (100 MHz, $CDCl_3$) δ 162.8, 156.1, 118.8, 115.4, 102.0, 80.8, 75.0, 73.2, 71.0, 70.8, 70.4, 70.1, 69.9, 68.5, 60.7, 58.9, 55.0−53.4 (unresolved signals), 51.8; IR (KBr) $\tilde{\nu}$ 2863, 2202 (CN), 1598, 1562, 1521, 1470, 1347, 1265, 1122 cm^{-1}; APCIMS *m/z* 827 ($M^+ + 3$, 13), 826 ($M^+ + 2$, 47), 825 ($M^+ + 1$, 100), 594 (17), 440 (6), 386 (69), 251 (16), 149 (34). Anal. Calcd for $C_{42}H_{52}FeN_6O_8$: C, 61.16; H, 6.36; N, 10.19. Found: C, 60.99; H, 6.20; N, 10.05.

(*Z*)-5-{3-[1′-(1-Chlorovinyl)ferrocen-1-yl]-3-diethylaminoallylidene}-1,3-diethyl-2-thioxodihydropyrimidine-4,6(1*H*,5*H*)-dione 12. Diethylamine (0.1 mL, 0.968 mmol) was added to a solution of compound **6** (40 mg, 0.077 mmol) in CH_2Cl_2 (10 mL), and the mixture was stirred at room temperature for 10 min and then filtered, and the solvent was evaporated under reduced pressure. The residue was subjected to flash column chromatography (3 × 15 cm, silica, CH_2Cl_2/AcOEt 2:1) to give **12** (41 mg, 95%) as an orange solid (CH_2Cl_2/AcOEt), mp 157−158 °C; ^{1}H NMR (300 MHz, $CDCl_3$) δ 9.23 (d, 1H, J = 14.4 Hz), 7.88 (d, 1H, J = 14.4 Hz), 5.48 (s, 1H), 5.29 (s, 1H), 4.62 (m, 12H), 3.74 (m, 4H), 1.35 (m, 12H); ^{13}C NMR (75 MHz, $CDCl_3$) δ 178.1, 173.1, 162.5, 160.0, 153.3, 136.9, 111.2, 108.2, 99.8, 85.7, 74.9, 73.2, 72.8, 70.4, 47.5, 43.2−42.6 (unresolved signals), 13.1, 12.7; IR (KBr) $\tilde{\nu}$ 2975, 2925, 1629 (C═O), 1542, 1516, 1419, 1383, 1337, 1240, 1153, 1112 cm^{-1} (C═S); APCIMS *m/z* 556 ($M^+ + 3$, 38), 554 ($M^+ + 1$, 100), 518 ($M^+ -$ HCl, 7), 464 (47), 428 (18), 374 (15), 270 (9); UV−vis (10^{-5} M, CH_3CN) λ (ϵ) 441 (92113), 243 nm (34 040 M^{-1} cm^{-1}). Anal. Calcd for $C_{27}H_{32}ClFeN_3O_2S$: C, 58.54; H, 5.82; N, 7.59. Found: C, 58.49; H, 5.78; N, 7.53.

(*Z*)-5-{3-[1′-(1-Chlorovinyl)ferrocen-1-yl]-3-(1,4,7,10-tetraoxa-13-azacyclopentadec-13-yl)allylidene}-1,3-diethyl-2-thioxodihydropyrimidine-4,6(1*H*,5*H*)-dione 13. Na_2CO_3 (21 mg, 0.195 mmol) and 1,4,7,13-tetraoxa-10-azacyclopentadecane (17 mg, 0.077 mmol) in CH_2Cl_2 (1 mL) were added to a solution of compound **6** (20 mg, 0.039 mmol) in CH_2Cl_2 (2 mL), and the mixture was stirred at room temperature for 2.5 h and then filtered, and the solvent was evaporated under reduced pressure. The residue was subjected to flash column chromatography (3 × 20 cm, silica, CH_2Cl_2 to CH_2Cl_2/MeOH 8:2) to give **13** (26 mg, 96%) as an orange solid (CH_2Cl_2), mp 65−66 °C; ^{1}H NMR (300 MHz, $CDCl_3$) δ 9.12 (d, 1H, J = 13.6 Hz), 7.83 (d, 1H, J = 13.6 Hz), 5.49 (s, 1H), 5.30 (s, 1H), 4.70−4.59 (m, 12H), 4.01 (m, 4H), 3.88 (m, 4H), 3.66 (m, 12H), 1.30 (m, 6H); ^{13}C NMR (75 MHz, $CDCl_3$) δ 178.1, 173.9, 162.3, 161.4, 153.7, 136.9, 111.1, 108.7, 100.4, 85.6, 75.1, 73.3, 73.2, 71.0, 70.6, 70.2, 70.1, 68.5, 54.7, 43.0, 42.5, 12.6; IR (KBr) $\tilde{\nu}$ 2863, 1634 (C═O), 1537, 1378, 1260, 1153, 1112 cm^{-1} (C═S); APCIMS *m/z* 702 ($M^+ + 3$, 42), 701 ($M^+ + 2$, 36), 700 ($M^+ + 1$, 100), 520 (50), 149 (9); UV−vis (10^{-5} M, CH_3CN) λ (ϵ) 446 (118 874), 291 (23 445), 243 (41 210), 202 nm (43 727 M^{-1} cm^{-1}). Anal. Calcd for $C_{33}H_{42}ClFeN_3O_6S$: C, 56.62; H, 6.05; N, 6.00. Found: C, 56.56; H, 5.98; N, 5.94.

(*Z*),(*Z*)-1,1′-Bis[1-diethylamino-3-(1,3-diethyl-2-thioxo-4,6-(1*H*,5*H*)-dioxodihydropyrimidine-5-ylidene)allyl]ferrocene 14. Na_2CO_3 (16 mg, 0.136 mmol) and diethylamine (0.007 mL, 0.068 mmol) were added to a solution of compound **7** (20 mg, 0.028 mmol) in CH_2Cl_2 (3 mL), and the mixture was stirred at room temperature for 2 h and then filtered, and the solvent was evaporated under reduced pressure. The residue was subjected to flash column chromatography (3 × 20 cm, silica, CH_2Cl_2 to CH_2Cl_2/AcOEt 9:1) to give **14** (21 mg, 95%) as an orange solid (CH_2Cl_2), mp >250 °C; ^{1}H NMR (300 MHz, $CDCl_3$) δ 9.45 (d, 2H, J = 14.4 Hz), 7.84 (d, 2H, J = 14.4 Hz), 5.30 (s, 4H), 4.78 (s, 4H), 4.60 (m, 8H), 3.50 (m, 8H), 1.32−1.16 (m, 24H); ^{13}C NMR (75 MHz, $CDCl_3$) δ 177.9, 171.6, 162.6, 161.2, 150.8, 109.1, 99.4, 79.5, 75.9, 72.9, 71.1, 48.8, 43.1, 42.6, 12.7; IR (KBr) $\tilde{\nu}$ 2971, 2925, 1629 (C═O), 1542, 1424, 1388, 1357, 1342, 1260, 1239, 1117 cm^{-1} (C═S); APCIMS *m/z* 803 ($M^+ + 3$, 16), 802 ($M^+ + 2$, 30), 801 ($M^+ + 1$, 100), 591 (6), 375 (26); UV−vis (10^{-5} M, CH_3CN) λ (ϵ) 442 (115 974), 291 (12 764), 235 nm (25 469 M^{-1} cm^{-1}). Anal. Calcd for $C_{40}H_{52}FeN_6O_4S_2$: C, 59.99; H, 6.54; N, 10.49. Found: C, 60.06; H, 6.58; N, 10.42.

(*Z*),(*Z*)-1,1′-Bis[1-(1,4,7,10-tetraoxa-13-azacyclopentadec-13-yl)-3-(1,3-diethyl-2-thioxo-4,6(1*H*,5*H*)-dioxodihydropyrimidine-5-ylidene)allyl]ferrocene 15. Na_2CO_3 (16 mg, 0.136 mmol) and 1,4,7,13-tetraoxa-10-azacyclopentadecane (16 mg, 0.068 mmol) in CH_2Cl_2 (1 mL) were added to a solution of compound **7** (20 mg, 0.028 mmol) in CH_2Cl_2 (3 mL), and the mixture was stirred at room temperature for 20 h and then filtered, and the solvent was evaporated under reduced pressure. The residue was subjected to flash column chromatography (3 × 15 cm, silica, CH_2Cl_2 to CH_2Cl_2/MeOH 7:1) to give **15** (29 mg, 97%) as an orange solid (CH_2Cl_2), mp 203−204 °C; ^{1}H NMR (300 MHz, $CDCl_3$) δ 9.32 (d, 2H, J = 14.4 Hz), 7.78 (d, 2H, J = 14.4 Hz), 5.28 (s, 4H), 4.76 (s, 4H), 4.57 (m, 8H), 3.75−3.55 (m, 40H), 1.30 (m, 12H); ^{13}C NMR (75 MHz, $CDCl_3$) δ 178.0, 171.8, 162.5, 161.1, 151.2, 109.4, 100.1, 79.5, 76.1, 72.8, 70.8, 70.5, 70.0, 68.0, 55.6, 43.2, 42.6, 12.8, 12.6; IR (KBr) $\tilde{\nu}$ 2873, 1629 (C═O), 1542, 1388, 1270, 1209, 1117 cm^{-1} (C═S); APCIMS *m/z* 1093 ($M^+ + 1$, 1), 879 (5), 521 (100); UV−vis (10^{-5} M, CH_3CN): λ (ϵ) 446 (132 437), 295 (16 311), 238 (27 054), 204 nm (35 480 M^{-1} cm^{-1}). Anal. Calcd for $C_{52}H_{72}FeN_6O_{12}S_2$: C, 57.13; H, 6.64; N, 7.69. Found: C, 67.07; H, 6.59; N, 7.63.

(*Z*),(*Z*)-2,14-Bis{3-(1,3-diethyl-2-thioxo-4,6(1*H*,5*H*)-dioxodihydropyrimidine-5-ylidene)-1-[1′-(1-chlorovinyl)ferrocen-1-yl]-1-propenyl}-1,15-diphenyl-2,14 -diaza-5,8,11-trioxapentadecane 17. Na_2CO_3 (57 mg, 0.54 mmol) in water (1 mL) and 1,15-diphenyl-2,14-diaza-5,8,11-trioxapentadecane **16**[31] (20 mg, 0.054 mmol) in THF (3 mL) were added to a solution of compound **6** (83 mg, 0.161 mmol), and the mixture was stirred at room temperature for 20 min, then poured on an aqueous solution of HCl (1M, 50 mL), and extracted with CH_2Cl_2 (2 × 40 mL), and the combined organic extracts were washed with H_2O and dried ($MgSO_4$), and the solvent was evaporated under reduced pressure. The residue was subjected

to flash column chromatography (3 × 20 cm, silica, CH_2Cl_2 to CH_2Cl_2/MeOH 20:1) to give **17** (32 mg, 44%) as an orange solid (CH_2Cl_2), mp 83−84 °C; ^{1}H NMR (300 MHz, $CDCl_3$) δ 9.11 (d, 2H, J = 14.4 Hz), 7.90 (d, 2H, J = 14.4 Hz), 7.36 (m, 6H), 7.14 (m, 4H), 5.49 (s, 2H), 5.15 (s, 2H), 4.65−4.58 (m, 28H), 3.77 (s, 8H), 3.60 (s, 8H), 1.33−1.25 (m, 12H); ^{13}C NMR (75 MHz, $CDCl_3$) δ 178.2, 174.6, 162.4, 161.3, 154.3, 136.8, 135.5, 129.2, 128.1, 127.0, 111.3, 108.4, 101.0, 85.7, 74.9, 73.3, 73.2, 70.6, 70.5, 70.0, 68.2, 57.9, 52.2, 43.2, 42.6, 12.6; IR (KBr) $\tilde{\nu}$ 2929, 1634 (C═O), 1532, 1378, 1255, 1193, 1112 cm^{-1} (C═S); APCIMS m/z 1335 (M^+ + 1, 4), 973 (12), 782 (18), 741 (21), 602 (32), 554 (57), 374 (45), 223 (100), 149 (55); UV−vis (10^{-5} M, CH_3CN) λ (ϵ) 446 (104 400), 286 (27 953), 240 nm (43 936 M^{-1} cm^{-1}). Anal. Calcd for $C_{68}H_{74}Cl_2Fe_2N_6O_7S_2$: C, 61.22; H, 5.59; N, 6.30. Found: C, 61.16; H, 5.53; N, 6.25.

Acknowledgment. We gratefully acknowledge financial support from the Dirección General de Investigación of Spain (Projects CTQ2005-07562-C04-02/BQU and CTQ2006-15456-C04-04/BQU) and Junta de Castilla y León, Consejería de Educación y Cultura, y Fondo Social Europeo (Project BU013A06).

Supporting Information Available: General experimental procedures, colorimetric studies, and titration of compounds. UV−vis spectra of **12**−**13**, **15**, and **17** in the presence of cations. Determination of complex formation constants of **12**−**14** and **17** against [Cu^{2+}]. UV−vis titration and titration profiles of **12**−**15** and **17** against [Hg^{2+}] and [Fe^{3+}]. ^{1}H NMR titration spectra of **14**, **15**, and **17** against [Cu^{2+}]. Determination of complex formation constants of **14**, **15**, and **17** in the presence of benzoate, acetate, and cyanide anions. ^{1}H NMR spectra of the titration of **17** against [CN^-]. ^{1}H NMR spectra of **2** and **3** and ^{1}H and ^{13}C NMR spectra of **4**−**15** and **17**. This material is available free of charge via the Internet at http://pubs.acs.org.

JO0702589